

Significant formation of sulfate aerosols contributed by the heterogeneous drivers of dust surface

Tao Wang¹, Yangyang Liu¹, Hanyun Cheng¹, Zhenzhen Wang¹, Hongbo Fu¹, Jianmin Chen¹, Liwu Zhang^{1,2*}

5 1 Shanghai Key Laboratory of Atmospheric Particle Pollution and Prevention, National Observations and Research Station for Wetland Ecosystems of the Yangtze Estuary, IRDR international Center of Excellence on Risk Interconnectivity and Governance on Weather, Department of Environmental Science & Engineering, Fudan University, Shanghai, 200433, Peoples' Republic of China

2 Shanghai Institute of Pollution Control and Ecological Security, Shanghai, 200092, Peoples' Republic of China

10 *Correspondence to:* Liwu Zhang (zhanglw@fudan.edu.cn)

Abstract. The importance of dust heterogeneous chemistry in the removal of atmospheric SO_2 and formation of sulfate aerosols is not adequately understood. In this study, the Fe, Ti, Al-bearing components, Na^+ , Cl^- , K^+ , and Ca^{2+} of the dust surface were discovered to be closely associated with the heterogeneous formation of sulfate. Regression models were then developed to make a reliable prediction for the heterogeneous reactivity based on the particle chemical compositions. Further,

15 the recognized gas-phase, aqueous-phase and heterogeneous oxidation routes were quantitatively assessed and kinetically compared by combining the laboratory work with modeling study. In the presence of $55 \mu\text{g m}^{-3}$ airborne dust, heterogeneous chemistry accounts for approximately 28.6% of the secondary sulfate aerosols during nighttime, while the proportion decreases to 13.1% in the presence of solar irradiation. On the dust surface, heterogeneous drivers (e.g. transition metal constituents,

20 water-soluble ions) are more efficient than surface adsorbed oxidants (e.g. H_2O_2 , NO_2 , O_3) in the conversion of SO_2 , particularly during nighttime. Dust heterogeneous chemistry offers an opportunity to explain the missing sulfate source during severe haze pollution events, and its contribution proportion in the complex atmospheric environments could be even higher than the current calculation results. Overall, the dust surface drivers are responsible for the significant formation of sulfate aerosols and have profound impacts on the atmospheric sulfur cycling.

1 Introduction

25 As an important component of atmospheric particulate matters, sulfate exerts profound impacts on the Earth's climate system, air quality, and public health (Seinfeld and Pandis, 2016; Wang et al., 2021a). The rapid formation of sulfate was proven as largely responsible for London Fog and Beijing Haze (Wang et al., 2016; Cheng et al., 2016). Secondary sulfate aerosols originate predominately from the oxidation of sulfur dioxide (SO_2) obeying the laws of gas-phase chemistry in gaseous environments, aqueous-phase chemistry in liquid media, and heterogeneous chemistry on aerosol surfaces (Ravishankara, 1997; 30 Mauldin III et al., 2012; Su et al., 2020; Liu et al., 2021a). In recent years, the newly discovered sulfate formation pathways were kinetically compared with the documented ones to evaluate the relative importance of them (Cheng et al., 2016; Gen et al., 2019; Liu et al., 2020; Wang et al., 2020a). Additionally, the oxidation channels in mainstream were compared by aerosol observation or modeling investigations (Berglen et al., 2004; Sarwar et al., 2013; He et al., 2018; Ye et al., 2018; Fan et al., 2020; Tao et al., 2020; Zheng et al., 2020; Song et al., 2021; Tilgner et al., 2021; Liu et al., 2021b; Wang et al., 2022a). These 35 studies emphasized the importance of the aimed liquid reaction or compared the sulfate contributions of diverse gas- and aqueous-phase pathways. Nevertheless, heterogeneous reaction was scarcely involved in the relevant discussions, thereby hindering the deeper understanding of the atmospheric gas-solid interactions.

40 Heterogeneous reaction alters the concentrations of gas-phase SO_2 and particle-phase sulfate, and its atmospheric influences were considered by observation and modeling works (Fairlie et al., 2010; Alexander et al., 2012; Chen et al., 2017; Wang et al., 2021b). As summarized by Table S1, when simulating the sulfate burst events, researchers observed the positive feedbacks after implementing heterogeneous chemistry into the WRF-Chem (Li et al., 2017), GEOS-Chem (Shao et al., 2019), CAMx (Huang et al., 2019) and CMAQ (Zhang et al., 2019a) models. However, these improved models highlighted the heterogeneous chemistry motivated by the surface adsorbed oxidants rather than the heterogeneous drivers of aerosol surface. To address the 45 knowledge gap, the revised GEOS-Chem (Wang et al., 2014) and WRF-CMAQ (Zheng et al., 2015) models considered the heterogeneous oxidation driven by aerosol surfaces, and successfully reproduced the rapid sulfate formation. Xue et al. (2016) moved forward to develop an observation-based model and found that heterogeneous chemistry contributed up to one third of the secondary sulfate in a typical haze-fog event. However, the "aerosol surface" mentioned in the previous works was not distinguished by its physical or chemical properties (Wang et al., 2014; Zheng et al., 2015; Xue et al., 2016), thereby making it difficult to compare the atmospheric importance of the diverse airborne surfaces. As discussed above, it is of great importance 50 to investigate the heterogeneous drivers of one selected aerosol surface, and further evaluate the atmospheric significance of the heterogeneous chemistry.

55 The resurgence of sandstorms in North China makes the air pollution situation more complex than ever before. The concentration of PM_{10} (particulate matter with an aerodynamic diameter of less than ten micrometers) in Beijing reached up to $3600 \mu\text{g m}^{-3}$, largely beyond the standards of World Health Organization and Chinese government (Li et al., 2021). As the most abundant primary aerosol in the troposphere (Textor et al., 2006; Tang et al., 2016), dust particles could transport more

than one full circuit around the globe within \sim 2 weeks (Uno et al., 2009) and concurrently participate into an array of atmospheric reactions. Heterogeneous reactions over dust surface consume and produce various trace gases, thereby affecting the dust property and tropospheric oxidation capacity (Tang et al., 2016). One of the most extensive concerns is that the numerous surface sites of windblown dust provide opportunities for a variety of atmospheric reactions to occur, e.g. oxidation of SO_2 and formation of sulfate (Usher et al., 2003). In the past decades, plenty of laboratory works have been performed to explore the heterogeneous behaviors of SO_2 on dust surfaces.

When discussing the heterogeneous chemistry on dust proxies, environmental factors including humidity, temperature, irradiance were frequently concerned. Adsorbed water accelerates the hydration of SO_2 but also competes with SO_2 for surface sites (Rubasinghe and Grassian, 2013). The exothermic adsorption of SO_2 results in the negative temperature dependence (Clegg and Abbatt, 2001a), except for the positive effects observed below 250K (Wu et al., 2011) or during the initial reaction stage (Wang et al., 2018a). Light irradiation normally accelerates the transformation of (bi)sulfites to (bi)sulfates (Li et al., 2010; Nanayakkara et al., 2012; Han et al., 2021), while iron oxides may undergo photoreactive dissolution and reflect negative light effect (Fu et al., 2009). The reactivity can be enhanced by H_2O_2 (Huang et al., 2016), or O_3 (Li et al., 2006; Li et al., 2007; Zhang et al., 2018), or NO_x (Ma et al., 2008; Liu et al., 2012; He et al., 2014; Yu et al., 2018; Zhao et al., 2018; Yang et al., 2018a; Wang et al., 2020b), or NH_3 (Yang et al., 2016; Yang et al., 2018b; Yang et al., 2019), or Cl_2 (Huang et al., 2017). By contrast, organic compounds, like CH_3CHO (Zhao et al., 2015), HCOOH (Wu et al., 2013), CH_3COOH (Yang et al., 2020; Wang et al., 2022b) and C_3H_6 (Chu et al., 2019), were found to suppress the interactions due to the accumulation or production of particle-phase organic acids. In terms of particle property, size (Baltrusaitis et al., 2010; Zhang et al., 2016), morphology (Li et al., 2019) and crystal structure (Yang et al., 2017) exhibit varied impacts. Among the common mineral constituents, Fe_2O_3 is more efficient than Al_2O_3 and SiO_2 (Chughtai et al., 1993; Zhang et al., 2006; He et al., 2014). Moreover, the addition of moderate nitrate (Kong et al., 2014; Du et al., 2019), or surfactant (Zhanzakova et al., 2019), or Al_2O_3 (Wang et al., 2018b) into the dust community could favor the heterogeneous uptake of SO_2 . Relative to the environmental factors, the heterogeneous effects relevant to particle property are still under debate.

The usage of simple mineral oxide as a substitution for natural dust may be problematic as such approach could undermine the atmospheric importance of more complex mineralogy. Authentic dusts were utilized in laboratory works (Table S2). Some studies concerned single samples like Saharan dust (Ullerstam et al., 2002; Ullerstam et al., 2003; Adams et al., 2005; Harris et al., 2012), Arizona test dust (Park and Jang, 2016; Zhang et al., 2019a; Zhang et al., 2019b), China loess (Usher et al., 2002) and Asian dust (Ma et al., 2012). The comparison of diverse samples has been attracting increasing attention. Zhou et al. (2014) observed the positive temperature effect on Xinjiang sierozem, in contrast to the negative temperature dependence for Inner Mongolia desert dust. Huang et al. (2015) discovered the accelerated oxidation of SO_2 by H_2O_2 , and attributed the different moisture effects to the dusts' varying components. Maters et al. (2017) explored the heterogeneous uptake on volcanic ash and glass samples, and related the reactivity differences to the varying abundances of surface basic and reducing sites. Park et al. (2017) compared the heterogeneous reactions on Gobi desert dust and Arizona test dust, and linked the sulfate formation to the quantity of semi-conductive metals. Wang et al. (2019) discovered the enhanced uptake of SO_2 on clay minerals after the

90 simulated cloud processing, and explained this evolution by the modification of iron speciation. Urupina et al. (2019) discussed the kinetics of diverse volcanic dusts, and further experimentally proved that neither one selected pristine oxide nor a mixture of them can adequately typify the behavior of natural dust (Urupina et al., 2021). Recently, based on the measurement method for sulfite and sulfate (Urupina et al., 2020), they determined the associations between sulfate production and dust chemical properties like (Fe+Al)/Si and Na abundance (Urupina et al., 2022). The aforementioned works broaden the horizons of the
95 heterogeneous drivers on dust surface. Up to now, the dominate dust surface drivers remain controversial due to the limited statistical linkages between the chemical composition of dust and the production rate of sulfate.

While the atmospheric relevance of the oxidation of SO_2 on dust has been widely recognized (Wu et al., 2020; Xu et al., 2020), the contribution of dust heterogeneous chemistry to secondary sulfate aerosols has not been quantitatively determined. By means of the improved WRF-CMAQ model, Wang et al. (2012) attributed a 27% decrement of SO_2 concentration and a 12%
100 increment of sulfate concentration to the heterogeneous chemistry during an Asian dust storm. Moreover, Tian et al. (2021) recently simulated the heterogeneous formation of dust sulfate by the revised GEOS-Chem model and found that, during the dust episodes in North China, up to 30% of the secondary sulfate resulted from the heterogeneous chemistry on dust surface. However, the photocatalytic reactivity of dust was not considered by the advanced models. Yu et al. (2017) developed the atmospheric mineral aerosol reaction (AMAR) model based on the laboratory works, and suggested that the heterogeneous
105 photocatalysis of mineral dust surface contributed more than half of the secondary sulfate. However, the heterogeneous reactivity was measured by quantifying all of the adsorbed SO_2 rather than calculating the yield of particle-phase sulfate. Moreover, limited gas- and aqueous-phase pathways were included in these models, and the heterogeneous reactivities of surface adsorbed oxidants and dust surface drivers have not been distinguished yet. Therefore, it is highly desirable to comprehensively compare the dust heterogeneous chemistry with other documented sulfate formation pathways.

110 Hereby, upon understanding the driving factors and driving force of the airborne dust surface, this work compared dust heterogeneous chemistry with gas- and aqueous-phase chemistries with respect to the formation rate of sulfate and atmospheric lifetime of SO_2 . In order to characterize the sensitivity of heterogeneous reaction to dust loading, the scenarios with different dust concentrations were also considered. The joint influences of ionic strength and aerosol liquid water content on the aqueous-phase oxidation of SO_2 were further discussed to prove the significance of heterogeneous kinetics under diverse
115 atmospheric conditions. The recently reported interfacial oxidations were additionally compared with the heterogeneous chemistry to emphasize the atmospheric relevance of dust surface drivers. This study attempted to verify the significant formation of sulfate aerosols contributed by the heterogeneous drivers of dust surface.

2 Methods

2.1 Technique route

120 This study attempted to investigate whether the heterogeneous oxidation of SO_2 on dust surface, particularly that induced by the dust surface drivers, makes great impacts on the loss of gaseous SO_2 and formation of sulfate aerosols (Text S1, Fig. S1). The gas- and aqueous-phase pathways were assessed by the documented methodologies and parameterizations (Cheng et al., 2016; Seinfeld and Pandis, 2016; Shao et al., 2019; Song et al., 2021), as briefly introduced by Sect. 2.2 (more details in Supporting Information). The heterogeneous conversion of SO_2 comprises dust-mediated and dust-driven modes, emphasizing the oxidants co-adsorbed with SO_2 and the drivers of dust surface, respectively. In the dust-mediated mode, dust surface functions as a reaction medium supporting the interactions between adsorbed oxidants and SO_2 . In the dust-driven mode, the oxidation of adsorbed SO_2 is initiated by the active components of dust surface. The former mode was assessed by the particle properties based on the reported methodology, while the later mode was quantitatively characterized by the laboratory works.

2.2 Gas- and aqueous-phase chemistries

130 The gas-phase oxidation of SO_2 is initiated by hydroxyl radical (OH), stabilized Criegee intermediates (CIs) and nitrate radical (NO_3). The former two oxidants promote the sulfate formation during daytime, while the latter one works mainly during nighttime. More details can be found in Text S2.

135 The aqueous-phase sulfate formation is pH-dependent and can be quantified based on the published documents and the references cited therein (Cheng et al., 2016; Su et al., 2020; Liu et al., 2021a). Herein, aqueous-phase chemistry refers to the liquid SO_2 conversion accelerated by the transition-metal ion-catalyzed oxygen (TMI- O_2), ozone (O_3), hydrogen peroxide (H_2O_2), nitrogen oxide (NO_2), methyl hydroperoxide (CH_3OOH), peroxyacetic acid (CH_3COOOH), hypochlorous acid (HOCl), hypobromous acid (HOBr), dissolved nitrous acid (HONO), as well as the photosensitization and nitrate photolysis only considered for daytime. More details can be found in Text S3 and Tables S3-S4.

140 The oxidant concentration data were derived from the atmospheric observation campaigns performed in Beijing, North China.

145 The measurements in warm seasons were considered in priority to correspond the experimental temperature of this study. Considering the relatively high irradiance used in the laboratory experiments, the oxidant parameters for daytime discussion were selected from the observations performed at noon time. The influences of dust loading on the oxidant concentrations, nitrate photolysis kinetics and TMI abundances were considered to reflect the linkages between different reactions. More details can be found in Text S4 and Table S5.

2.3 Heterogeneous chemistry-particle characterizations

Five airborne clay minerals, including Nontronite (NAu), Chlorite (CCa), Montmorillonite (SWy), Kaolin (KGa) and Illite (IMt), were obtained from the Source Clay Minerals Repository (Purdue University, West Lafayette, Indiana, USA). The

145 purchased clays were sent for the following measurements.

150 The clay minerals were analyzed by X-ray fluorescence spectrometer (Axios Advanced, PANalytical, Netherlands) for element distributions (Table S6). The Brunauer-Emmett-Teller (BET) specific surface areas (SBET) of NAu, CCa, SWy, KGa and IMt were measured by a Quantachrome Nova 1200 BET apparatus to be 19.76, 5.67, 22.64, 18.77 and 20.05 m² g⁻¹, respectively. Particles were suspended in Milli-Q water (18.2 MΩ.cm at 25 °C) before the size measurement (ViewSizerTM 3000, MANTA Instruments, USA). The particle diameters range mostly from 50 to 1000 nm and are averaged to be 399 nm for NAu, 272 nm for CCa, 438 nm for SWy, 396 nm for KGa, and 366 nm for IMt (Fig. S2).

155 Particles were ultrasonically extracted in Milli-Q water, followed by the filtration through a polytetrafluoroethylene membrane filter. The obtained solution was analyzed by an ion chromatography (883 Basic, Metrohm, Switzerland) for the concentrations of anions (HCOO⁻, Cl⁻, NO₃⁻, SO₄²⁻) and cations (Na⁺, NH₄⁺, K⁺, Mg²⁺, Ca²⁺) (Fig. S3) by the reported methods (Wang et al., 2020c). The water-soluble ions account for 4.6%, 0.1%, 8.5%, 0.3% and 0.8% of the mass contents of NAu, CCa, SWy, KGa and IMt, respectively.

160 A mixture, denoted as natural dust hereafter, was prepared by mechanically mixing the studied clay minerals by their atmospheric abundances. Because the clays in Kaolinite group (NAu, KGa), Montmorillonite group (SWy), Illite group (IMt) and Chlorite group (CCa) occupy respectively 6.6%, 4.0%, 53.8% and 4.3% mass fractions of the airborne dust (Usher et al., 2003), the prepared natural dust sample comprises 8.8 wt% of NAu, 8.8 wt% of KGa, 5.3 wt% of CCa, 71.4 wt% of IMt, and 5.7 wt% of CCa.

165 2.4 Heterogeneous chemistry-DRIFTS measurements

170 The *in-situ* DRIFTS (diffuse reflectance infrared Fourier transform spectroscopy) spectra were collected using a FTIR spectrometer (Tracer-100, Shimadzu, Japan) equipped with a mercury-cadmium-telluride detector cooled by liquid nitrogen. A gas supply system was constructed by linking the experimental units through Teflon tubes. Mass flow controllers (D07-19, Severstar, China) adjusted the reactant gases to the expected reactant concentration and relative humidity (RH). Gas cylinders: high-pure air (79% N₂ and 21% O₂), SO₂ (2.46×10^{15} molecules cm⁻³ diluted by N₂).

175 Before each experiment, a ceramic cup holding particles was placed into the reaction chamber. The particles were treated in a stream of dry air (300 ml min⁻¹) for 30 min to minimize the surface water and impurities (Wang et al., 2018a, 2018c). After the pretreatment, the sample was exposed to humidified air (RH = 50%) to reach moisture saturation, followed by the collection of background spectrum and then the introduction of reactant gas for 240 min. The SO₂ concentration was 3.69×10^{13} molecules cm⁻³ in a total flow rate of 100 ml min⁻¹.

180 The simulated solar irradiation with an actinic flux of 6.51×10^{15} photons cm⁻² s⁻¹ was provided by an Xenon lamp (TCX-250, Ceaulight, China). The reaction temperature (296.8K) was controlled by a heater attached to a recirculating cooling water system and determined by a calibration curve introduced previously (Wang et al., 2018a). The gas- and aqueous-phase parameters were correlated by the experimental temperature. All of the exposures were performed in triplicates. The experimental setups are displayed by Fig. S4, and the recorded spectra are shown in Fig. S5 and S6.

2.5 Heterogeneous chemistry-acidity and kinetics

The recorded spectra were analyzed by referring to the previous literatures and the references cited therein (Persson and Vgren, 1996; Peak et al., 1999; Goodman et al., 2001; Zhang et al., 2006; Wu et al., 2011; Liu et al., 2012; Nanayakkara et al., 2012; Nanayakkara et al., 2014; Huang et al., 2016; Ma et al., 2017; Yang et al., 2017). Totally six sulfur-containing species can be identified: hydrated SO_2 ($\text{SO}_2 \cdot \text{H}_2\text{O}$), bisulfite, sulfite, solvated sulfate, coordinated sulfate, bisulfate, and the assignments are summarized by Table S7. The overlapping bands were further analyzed by Gaussian/Lorentzian deconvolution to obtain the product distributions (Fig. S7). The consistent deconvolution procedure was performed for the infrared spectra derived from the repeated experiments.

Because part of the measured ions exist in the surface coordinated forms or crystalline states, the particle acidity (pH) may not be accurately characterized by the proxy methods (Hennigan et al., 2015). Herein, the ionization equilibrium of dissolved SO_2 in the water layers of particle surface is considered to be associated with particle acidity. As reported, the dissolved SO_2 would transform from $\text{SO}_2 \cdot \text{H}_2\text{O}$ to HSO_3^- , and then to SO_3^{2-} as the medium evolves from the extremely acidic to the nearly alkaline (Haynes, 2014; Zhang et al., 2015). The relative abundance of $\text{SO}_2 \cdot \text{H}_2\text{O}$ and SO_3^{2-} , as assumed to be equivalent to the relative integral area of their characteristic peaks, is utilized to calculate the particle acidity (more details in Text S3-2 of Supporting Information). The relative abundance of HSO_4^- and SO_4^{2-} , which can be used to calculate the aerosol acidity (Rindelaub et al., 2016; Ault, 2020), was not considered by the present study because the characteristic signals of bisulfate cannot be observed in some of the recorded infrared spectra.

Heterogeneous kinetics can be assessed by the reactive uptake coefficient (γ) by assuming a first-order loss of SO_2 . The γ for dust-driven heterogeneous chemistry can be calculated by:

$$\gamma = \frac{d[\text{SO}_4^{2-}]/dt}{Z} \quad (1)$$

$$Z = \frac{1}{4} \times A_s \times [\text{SO}_2] \times v_{\text{SO}_2} \quad (2)$$

$$v_{\text{SO}_2} = \sqrt{\frac{8RT}{\pi M_{\text{SO}_2}}} \quad (3)$$

Where $d[\text{SO}_4^{2-}]/dt$ is the rate of sulfate production on dust surface (ion s^{-1}), A_s is the reactive surface area (m^2), $[\text{SO}_2]$ is the experimental concentration of SO_2 (molecules m^{-3}), v_{SO_2} is the molecular velocity of SO_2 (m s^{-1}), R is gas constant ($\text{J mol}^{-1} \text{K}^{-1}$), T is the experimental temperature (K), M_{SO_2} is the molecular weight of SO_2 (kg mol^{-1}). Because the infrared intensity is proportional to the amount of surface product, $[\text{SO}_4^{2-}]$ can be translated by the integral area of the sulfate characteristic peaks:

$$[\text{SO}_4^{2-}] = f \times (\text{integral area}) \quad (4)$$

Where f is the conversion factor and represents the number of SO_4^{2-} corresponding to per unit integral area. The sulfate production rate of dust surface can be translated by the calibration curves by mixing weighed Na_2SO_4 with the target particle sample to a set of concentrations (Martin et al., 1987; Li et al., 2006; Wu et al., 2011; Wang et al., 2020d). The conversion

factors are calculated to be 1.32×10^{18} , 4.62×10^{17} , 6.97×10^{17} , 8.20×10^{17} , 9.44×10^{17} , and 9.25×10^{17} for NAu, CCa, SWy, KGa, IMt, and natural dust, respectively. Because the sulfate standard item was thoroughly mixed with the particles, S_{BET} was used to calculate the reactive uptake coefficient.

All of the particle samples except SWy presented steady sulfate production potentials over the entire experiment, while the products on SWy increased by reaction time in the beginning and then gradually remained unchanged (Fig. S8). Accordingly, the process on SWy was assessed by the experimental data of the first 30 min of reaction, and the kinetics of other samples were calculated by the spectra recorded throughout the experiment.

Besides the dust surface drivers, the heterogeneous conversion of SO_2 can be additionally initiated by the gaseous oxidants (O_3 , H_2O_2 , NO_2 , HOCl , HOBr , CH_3OOH , CH_3COOOH , HONO) co-adsorbed with SO_2 . Considering that the adsorption of oxidant onto dust surfaces would produce gas- and particle-phase species (Usher et al., 2003; Tang et al., 2017), the dust-mediated heterogeneous oxidation can be assumed to primarily proceed in the surface water layers. Such assumption can be experimentally proved as the acceleration of SO_2 oxidation induced by the co-oxidant (e.g. H_2O_2 , NO_2 , O_3) becomes more significant under higher humidity (Huang et al., 2015; Park et al., 2017; Zhang et al., 2018). Based on the previous studies (Hanson et al., 1994; Jacob, 2000; Shao et al., 2019), the γ for dust-mediated heterogeneous chemistry can be calculated by:

$$\gamma = \left[\frac{1}{\alpha} + \frac{v}{4H^*RT\sqrt{D_a k_{\text{chem}}}} \times \frac{1}{f_r} \right]^{-1} \quad (5)$$

$$k_{\text{chem}} = \frac{R_a}{\sum S_{(\text{IV})}} \quad (6)$$

$$f_r = \coth \frac{r_p}{l} - \frac{l}{r_p} \quad (7)$$

$$l = \sqrt{\frac{D_a}{k_{\text{chem}}}} \quad (8)$$

Where k_{chem} is the first-order reaction rate constant of the studied $S_{(\text{IV})}$ specie(s) (s^{-1}) that produce in the rate of R_a (M s^{-1}), f is the diffusive correction term comparing the radius of natural dust r_p (m) with the diffuse-reactive length l (m), α is the mass accommodation coefficient (dimensionless), D_a is the aqueous-phase diffusion coefficient of SO_2 ($1.78 \times 10^{-5} \text{ m}^2 \text{ s}^{-1}$ at 296.8 K) (Himmelblau, 1964; Haynes, 2014), H^* is the effective Henry's law constant for the studied $S_{(\text{IV})}$ specie(s) (M atm^{-1}), and R is gas constant ($\text{L atm mol}^{-1} \text{ K}^{-1}$).

The sulfate formation rate in the atmosphere can be calculated by the following equations (Jacob, 2000; Li et al., 2020a).

$$\frac{d[\text{SO}_4^{2-}]}{dt} = \left(\frac{r_p}{D_g} + \frac{4}{v\gamma} \right)^{-1} S_p [\text{SO}_2] \quad (9)$$

$$S_p = C \times F \times S_{\text{BET}} \quad (10)$$

Where $d[\text{SO}_4^{2-}]/dt$ is the atmospheric sulfate formation rate ($\mu\text{g m}^{-3} \text{ h}^{-1}$), r_p is the particle radius (m), D_g is the gas-phase diffusion coefficient of SO_2 ($\text{m}^2 \text{ h}^{-1}$), v is the molecular velocity of SO_2 (m s^{-1}), γ is the reactive uptake coefficient

(dimensionless), S_p is the particle surface area density ($\text{m}^2 \text{ m}^{-3}$), $[\text{SO}_2]$ is the atmospheric SO_2 concentration ($\mu\text{g m}^{-3}$), C is the dust concentration of $55 \mu\text{g m}^{-3}$ in representative of the common atmospheric condition of China (Zhang et al., 2012), F is the mass fraction of clay mineral in the natural dust community (%), S_{BET} is the BET specific surface area ($\text{m}^2 \text{ g}^{-1}$).

2.6 Atmospheric lifetime of SO_2

For the gas- and aqueous-phase pathways, the lifetime of SO_2 (τ) can be calculated by Eq. (11) (Jacob, 2000).

$$\tau = \frac{1}{k_{\text{chem}}} \quad (11)$$

Where k_{chem} is the assumed first-order reaction rate constant of the studied $\text{S}_{(\text{IV})}$ specie(s) (s^{-1}).

For the heterogeneous pathways, the τ can be calculated by Eq. (12) (Clegg and Abbatt, 2001b).

$$\tau = \frac{4}{\gamma v S_p} \quad (12)$$

Where γ is the reactive uptake coefficient (dimensionless), v is the molecular velocity of SO_2 (m s^{-1}), S_p is the particle surface area density ($\text{m}^2 \text{ m}^{-3}$), as described by Eq. (10).

The atmospheric lifetime caused by the multiple pathways (τ_{total}) can be estimated by Eq. (13) (Seinfeld and Pandis, 2016).

$$\tau_{\text{total}} = \left(\sum \frac{1}{\tau} \right)^{-1} \quad (13)$$

3 Results and discussion

3.1 Driving factors of dust surface

Correlation analysis was performed at first to explore the dominant surface drivers that affect the heterogeneous sulfate production on different clay minerals (Fig. 1a). Under dark condition, the sulfate production rate corrects positively with Fe, while presents negative dependence against Al. By means of aerosol mass spectrometer, airborne sulfate was reported to be highly associated with the iron-rich dusts, and the heterogeneous reaction of SO_2 was regarded as a plausible explanation (Sullivan et al., 2007). Conversely, Al_2O_3 presents weaker heterogeneous reactivity than Fe_2O_3 (Zhang et al., 2006; Yang et al., 2018b; Xu et al., 2021), and was proved to suppress the nocturnal heterogeneous reaction by blocking the reactive sites on other components (Wang et al., 2018b). Accordingly, Fe-bearing component plays a crucial role in the heterogeneous SO_2 oxidation, while the presence of Al-bearing component directly weakens the dust's reactivity or indirectly decreases the proportion of other active mineral constituents.

Recent studies proposed that transition metal oxides in dust act as photocatalyst that yields electron-hole pairs (Chen et al., 2012; Abou-Ghanem et al., 2020; Wang et al., 2020c; Sakata et al., 2021), followed by the formation of reactive oxygen species (ROS) including hydroxyl radical ($\cdot\text{OH}$), superoxide ($\text{O}_2^{\cdot-}$), hydroperoxyl radical (HO_2^{\cdot}) and dissociated active oxygen species (O^*). Sulfate radical ($\text{SO}_4^{\cdot-}$) is generated by the presence of abundant $\cdot\text{OH}$ and participates into the oxidation events (Antoniou et al., 2018; Kim et al., 2019; Li et al., 2020b). Hence, there is positive correlation between the content of Ti and the sulfate production enhanced by solar irradiation. The abundance of Al associates positively with the photoinduced sulfate enhancement as well. Physically, Al-bearing components disperse other efficient mineralogical constituents in case of agglomeration (Darif et al., 2016). Chemically, sunlight was found to alter the electronic configuration of $\alpha\text{-Al}_2\text{O}_3$, which presented photoactivity in the reported heterogeneous process (Guan et al., 2014). Hence, the discrepancy between the nocturnal and diurnal sulfate formation rates is primarily related to the existence of Ti- and Al-bearing mineral constituents.

No correlation can be observed between the abundance of element and the sulfate production rate of photoreaction. The dust sample with higher proportion of elemental Ti was reported to exhibit greater reactivity toward SO_2 (Park et al., 2017), or NO_2 (Ndour et al., 2009), or O_3 (Abou-Ghanem et al., 2020) in the photochemistry processes. However, these results were derived from the qualitative comparison rather than the quantitative analysis as performed in this work. Analogous to the Al_2O_3 discussed above, semi-conductive metal exhibits dual behaviors in dark and light reactions. For instance, the iron oxide under dark condition owns great reactivity toward SO_2 , whereas that under solar irradiation may present impaired heterogeneous kinetics due to its dissolution process (Fu et al., 2009). In addition, the heterogeneous reaction on the surface of TiO_2 or Ti-bearing mineral is thermodynamically favored during nighttime but largely dependent on photocatalysis under solar irradiation (Chen et al., 2012). Due to the complexity of photoreaction that involves both of the dark and light reaction mechanisms, the sulfate formation rate of photoreaction may not be directly linked to particle chemical compositions.

Some water-soluble ions (Na^+ , Cl^-) are observed to present positive impacts on the production of surface sulfate under dark

condition. The presence of halite (NaCl) has positive implications for the dust's hydroscopic property and may facilitate its heterogeneous reactivity (Wang et al., 2014; Tang et al., 2019). Moreover, there are negative associations between the photoinduced sulfate enhancement and the abundances of Na^+ , K^+ , Ca^{2+} . These cations can be hydrolyzed by adsorbed water to produce H^+ , thereby elevating the particle acidity. The increased acidity retards the hydrolysis and dissociation of SO_2 (Park et al., 2008; Huang et al., 2015), and inhibits the production of OH by the irradiated dust surfaces (Zheng et al., 1997; Yang et al., 2008; Liu et al., 2017a). Urupina et al. (2022) recently reported the positive correlations between secondary dust sulfate and the amount of elemental Na. The results here provide additional insights into the heterogeneous effects of the water-soluble constituents on dust surface.

The correlation analysis helps to quantitatively identify the dust surface drivers and better understand the reaction mechanism of dust heterogeneous chemistry. Regression analysis can be further performed to predict the surface kinetics by the chemical compositions of dust. Referring to the publication of Zhang et al. (2020), we derived an exponential parameterization for the production rate of particle-phase sulfate:

$$\text{SF}_{\text{dark}} = M[A]^a[B]^b[C]^c[D]^d[E]^e[F]^f + N \quad (14)$$

Where SF_{dark} is the yield of SO_4^{2-} on the particle sample of per unit mass within per unit time (ions $\text{g}^{-1} \text{s}^{-1}$); [A], [B], [C], [D], [E] and [F] are the mass fractions of element and ion (%); M and N are the constant parameters (dimensionless). After the statistical procedures by SPSS (version 22.0), we obtained the regression equation for the nocturnal heterogeneous reaction:

$$\text{SF}_{\text{dark}} (\times 10^{15}) = 22.858 [\text{Al}]^{-0.001} [\text{Fe}]^{0.111} [\text{Cl}^-]^{0.001} [\text{Na}^+]^{0.001} - 13.404 \quad (15)$$

Analogously, the discrepancy between the nocturnal and diurnal sulfate production rates, denoted as $R_{\text{light/dark}}$, can be described by:

$$R_{\text{light/dark}} = \text{SF}_{\text{light}} / \text{SF}_{\text{dark}} = 14.539 [\text{Al}]^{0.073} [\text{Ti}]^{0.167} [\text{Cl}^-]^{-0.001} [\text{Na}^+]^{-0.001} [\text{K}^+]^{-0.001} [\text{Mg}^{2+}]^{-0.001} - 3.186 \quad (16)$$

Then,

$$\text{SF}_{\text{light}} = \text{SF}_{\text{dark}} \times R_{\text{light/dark}} \quad (17)$$

Because the abundance variation of water-soluble ion presents significantly less influence on the prediction result relative to the elemental transition metal, the complete regression models can be simplified by merely considering the mineral element abundances:

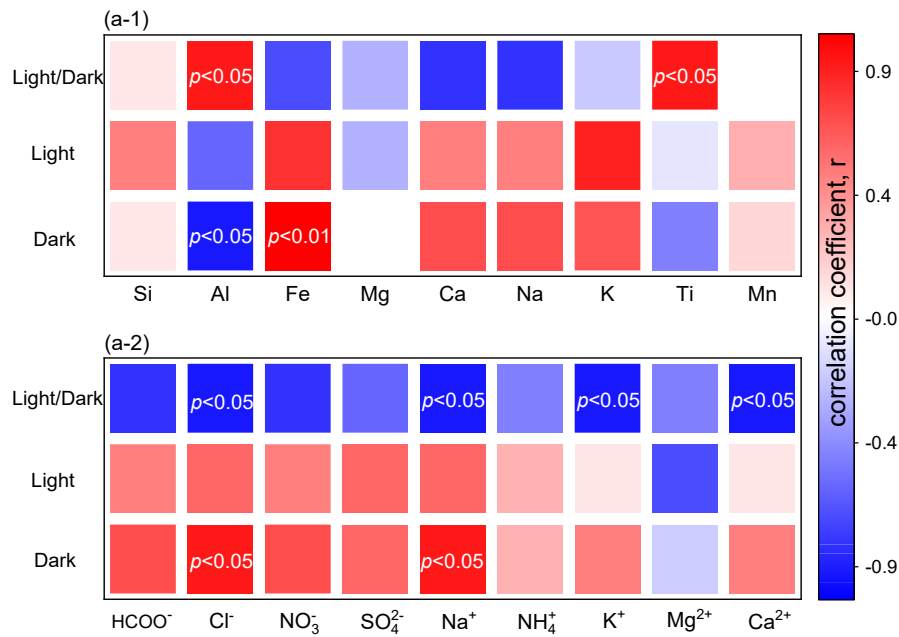
$$\text{SF}_{\text{dark}} (\times 10^{15}) = 30.880 [\text{Fe}]^{0.077} - 21.679 \quad (18)$$

$$R_{\text{light/dark}} = 15.581 [\text{Al}]^{0.062} [\text{Ti}]^{0.141} - 4.277 \quad (19)$$

$$\text{SF}_{\text{light}} = \text{SF}_{\text{dark}} \times R_{\text{light/dark}} \quad (20)$$

Both of the complete and simplified regression models accurately simulate the experimental data with all of the linear slopes approaching 1.0 and all of the R^2 values larger than 0.995 (Fig. 1b and c). The simplified regression model can be considered as the preferred recommendation due to the fewer parameters needed and its greater performance in the photoreaction prediction. Shang et al. (2010) found that the heterogeneous sulfate production on pristine TiO_2 (Degussa P25) can be accelerated by 8.4 times by the presence of ultraviolet light (365 nm, $350 \mu\text{W cm}^{-2}$). Such photoinduced enhancement is

comparable with the prediction result (10.2 times) derived from the simplified regression model developed by this study. Additionally, because the chemical composition of bulk sample may not fully explain the sulfate formation over dust surface, further study to discuss the model uncertainty is warranted.



320

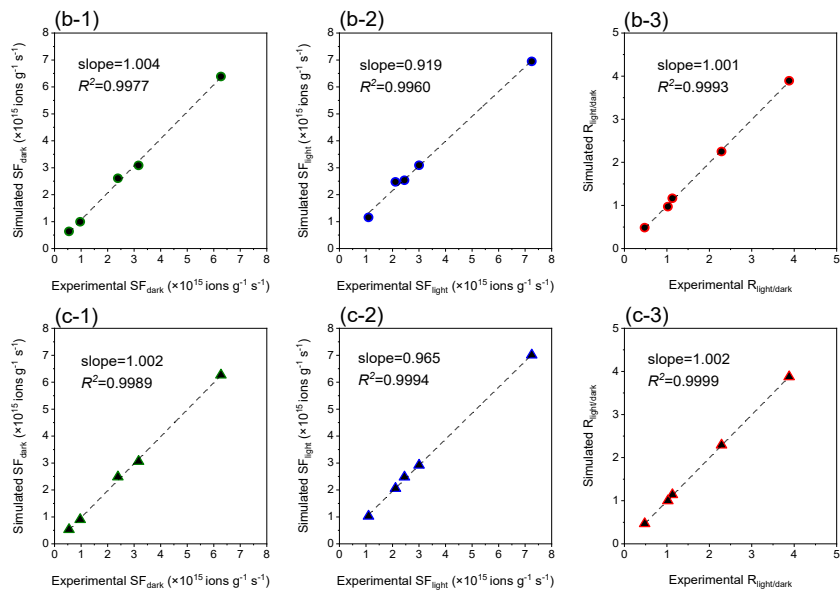


Figure 1. Correlation and regression analysis on the sulfate production rate of dust surface.

Correlation analysis bridging the rate of sulfate production and the abundance of (a-1) mineral element and (a-2) water-soluble ion. Linear relationships between the experimental SF_{dark}, SF_{light}, R_{light/dark} and those simulated by the (b) complete and (c) simplified regression models. The unit of SF (ions $\text{g}^{-1} \text{s}^{-1}$) indicates the number of SO₄²⁻ formed on the particle sample of per unit mass within per unit time, and R_{light/dark} indicates the ratio of SF values in presence and absence of simulated solar irradiation.

325

3.2 Driving force of dust surface

The driving force of dust surface can be characterized by reactive uptake coefficient and particle acidity (Fig. 2, Table S8).

330 Under dark condition, the reactive uptake coefficients are highest for SWy and NAu, followed by IMt and CCa, with that of KGa being the lowest. The presence of simulated solar irradiation causes a different rank: IMt>SWy>CCa>NAu>KGa. The diurnal uptake coefficients of CCa, SWy, KGa, IMt are respectively 1.52, 1.01, 2.94, 2.30 times greater than the corresponding nocturnal ones, reflecting the distinct photocatalytic performances of the clay minerals. Conversely, NAu presents the decreased heterogeneous uptake capacity under light irradiation than dark condition due to its rich abundance of Fe, whose 335 oxide species may occur photoreductive dissolution in acidic media (Fu et al., 2010; Shi et al., 2012). Comparing the studies performed by the same experimental approach and assessment procedures, the studied clay minerals are more efficient than the previously concerned mineral dust proxies, including CaCO_3 (Li et al., 2006; Wu et al., 2011; Zhang et al., 2018), Al_2O_3 (Liu et al., 2017b), TiO_2 (He and Zhang, 2019) and manganese oxides (Wang et al., 2020d), in the heterogeneous production of sulfate under the parallel conditions.

340 The reactive uptake coefficients for the natural-dust-driven heterogeneous chemistry were calculated to be 6.08×10^{-6} during nighttime and 1.14×10^{-5} during daytime (Fig. 2a). Within the data set of authentic dust, the nocturnal value is lower than those of China loess (3.0×10^{-5}), Inner Mongolia desert dust (2.41×10^{-5}), Xinjiang sierozem (8.34×10^{-5}), Saharan dust (6.6×10^{-5}), Asian mineral dust (2.54×10^{-5}), Tengger desert dust (4.48×10^{-5}) and ATD (1.92×10^{-5}) under the similar experimental conditions (Usher et al., 2002; Adams et al., 2005; Zhou et al., 2014; Huang et al., 2015). It should be noted that, the previous 345 studies measured net uptake coefficient that quantifies all of the heterogeneously adsorbed SO_2 , and some of them assessed the oxidation events accelerated by the surface adsorbed oxidants (e.g. NO_2 , O_3 , H_2O_2). In order to quantify the driving force of dust surface drivers in the contribution of particle-phase sulfate, S(IV) species were not considered for the kinetics calculation in this study. Quantitatively, the dust surface drivers are responsible for the atmospheric sulfate formation rates of 0.195 and $0.365 \mu\text{g m}^{-3} \text{ h}^{-1}$ during nighttime and daytime, respectively.

350 Particle acidity is another important index reflecting the impacts of dust heterogeneous chemistry. After the exposure to SO_2 , CCa is the most acidic, followed by IMt, KGa and NAu, leaving SWy being more neutral. Because no significant correlations can be found between γ and pH, the absolute acidity level is largely dependent on the basic nature of dust. The lowest pH assigned to CCa can be explained by its highest content of elemental Mg relative to the other clays (see Table S6). The Mg-bearing constituents dissolve to be Mg^{2+} that can be further hydrolyzed by water to produce H^+ , thus accelerating the 355 acidification of particle (Park et al., 2008; Huang et al., 2015). For one clay mineral, its different acidities after dark and light reactions reflect the distinct heterogeneous kinetics. All of the studied clays, with the exception of NAu, become more acidic after the photoreaction than the dark reaction, which can be explained by the photoinduced SO_2 adsorption and sulfate production on these samples. The opposite situation of NAu coincides to the decreased heterogeneous kinetics over its surface by the presence of solar irradiation. Generally, the natural dust presents the particle acidity (pH) of 4.177 after dark reaction 360 and 4.405 after photoreaction (Fig. 2b). Such results locate within the acidity ranges of dust seeds (3.0-7.0) (Ault, 2020; Pye

et al., 2020) and haze aerosols (3.5-4.8) (Ding et al., 2019; Song et al., 2019), suggesting that the dust-driven heterogeneous process could affect aerosol acidity by a certain extent.

Figure 3 presents the pH-dependent reactive uptake coefficients for the natural-dust-mediated heterogeneous chemistry, accompanied with the experimental data of dust-driven heterogeneous chemistry. The sulfate formation mediated by dust surface is primarily affected by the surface adsorbed H_2O_2 below the nocturnal pH of 5.5 or the diurnal pH of 5.3. When the dust acidity exceeds the thresholds, dust-mediated chemistry would be kinetically dominated by NO_2 and O_3 during nighttime, or HOBr and HOCl during daytime. The γ of NO_2 , O_3 , HOCl , HOBr and CH_3COOOH presents positive dependence toward pH, in accordance with the evolution of the effective Henry's law constant for the studied sulfur species, as theoretically illustrated by Eq. (5). Generally, the dust-driven chemistry appears to be more efficient than the dust-mediated chemistry over the estimated pH range, and thus could account for more secondary sulfate aerosols. In the following sections, the oxidation of SO_2 mediated or driven by the surfaces of natural dust would be set as the typical examples of dust-mediated and dust-driven heterogeneous chemistries to compare with the widely reported gas- and aqueous-phase processes.

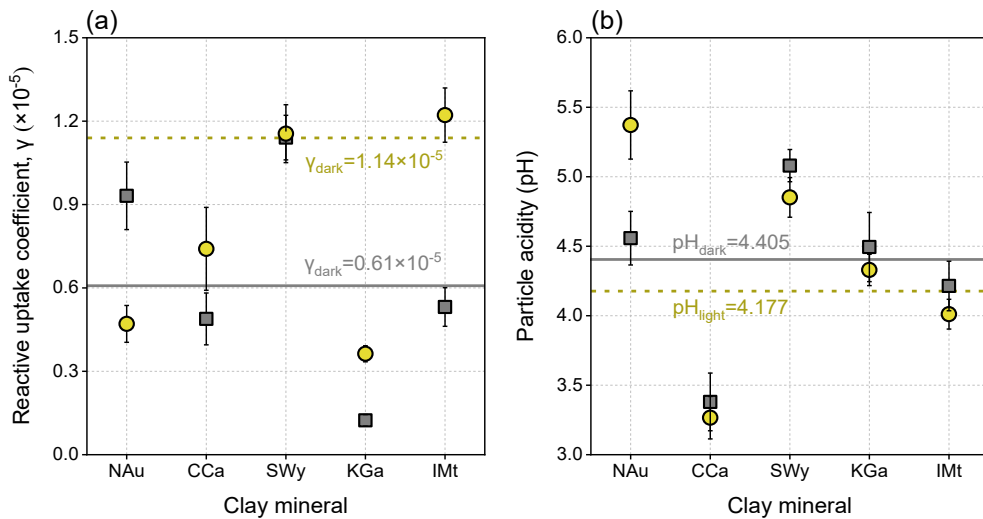
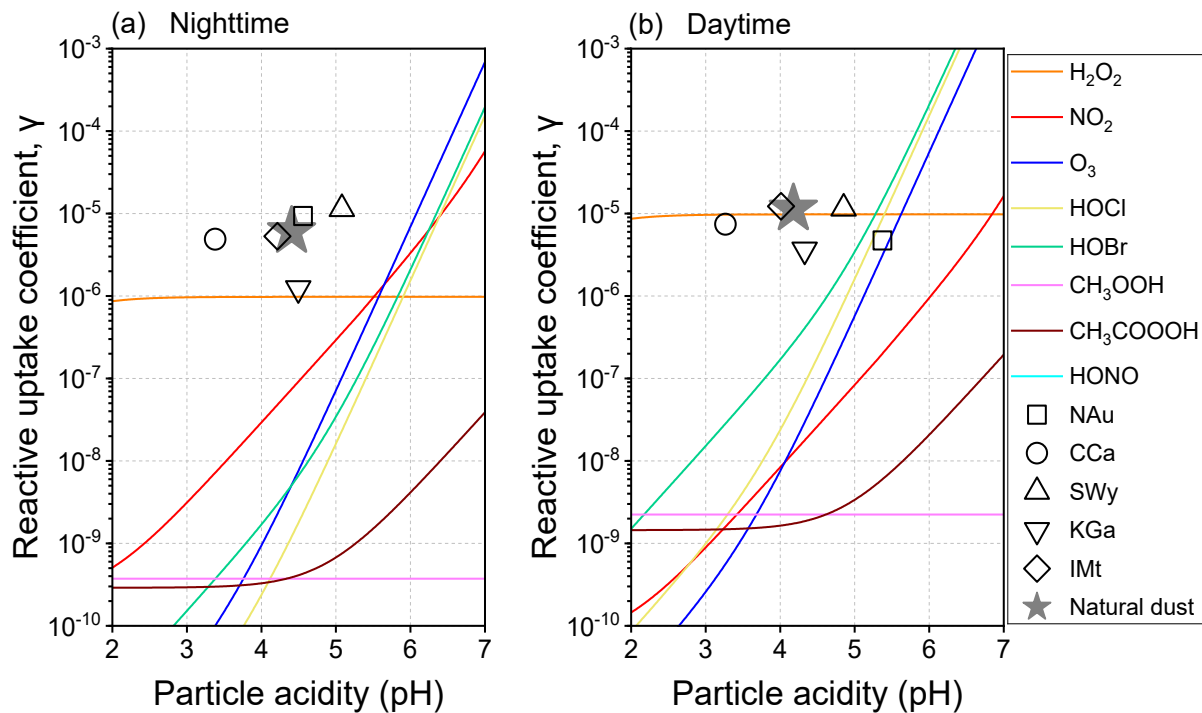


Figure 2. Analysis results of the *in-situ* infrared spectra recorded for the heterogeneous reaction of SO_2 on the clay minerals and natural dust.

(a) Reactive uptake coefficients (γ) for the heterogeneous production of sulfate. (b) Particle acidity (pH) after the heterogeneous reaction. Both of the dark (grey square) and light (yellow circle) conditions were considered. Dots represent the results of clay minerals, and those of natural dust are showed by the lines. All error bars represent 1 SD.



380

Figure 3. Particle-acidity-dependent reactive uptake coefficients for the dust-mediated and dust-driven heterogeneous sulfate formation.

385

The dust-mediated chemistry is induced by the surface oxidants co-adsorbed with SO_2 , including hydrogen peroxide (H_2O_2), nitrogen oxide (NO_2), ozone (O_3), hypochlorous acid (HOCl), hypobromous acid (HOBr), methyl hydroperoxide (CH_3OOH), peroxyacetic acid (CH_3COOOH) and dissolved nitrous acid (HONO). The dust-driven chemistry is induced by the heterogeneous drivers (transition-metal-bearing components and water-soluble ions) on the surfaces of natural dust and clay minerals [Nontronite (NAu), Chlorite (CCa), Montmorillonite (SWy), Kaolin (KGa), Illite (IMt)].

3.3 Comparison of atmospheric oxidation pathways

Figure 4 compares dust heterogeneous chemistry with the gas- and aqueous-phase pathways in terms of the atmospheric sulfate formation rate. The clay minerals are kinetically comparable with other reactive species (Fig. 4a and e), indicating that the dust-driven chemistry makes considerable contributions to secondary sulfate aerosols. For instance, during nighttime, the heterogeneous reactivity of IMt is only next to those of OH and TMI-O₂. The sulfate formation rates are summed to be 0.795 $\mu\text{g m}^{-3} \text{ h}^{-1}$ during nighttime and 5.179 $\mu\text{g m}^{-3} \text{ h}^{-1}$ during daytime by the parameterization scheme of this study. The elevated sulfate formation rate during daytime can be explained by the photo-increased oxidation channels, oxidant concentrations, heterogeneous reactivity, and the elevated particle acidity that facilitates the TMI catalysis. It is worthwhile to mention that, in the real atmosphere, the observed sulfate concentration during nighttime may be comparable to or exceed that during daytime, which can be explained by the higher nocturnal humidity facilitating the liquid oxidations or the lower boundary layer causing the adverse diffusion conditions (Liu et al., 2017c; Tutsak and Koçak, 2019; Li et al., 2020c). The relevant meteorological factors were not considered by this comparison model, and the current results emphasized the different sulfate formation potentials through kinetic regime. The sulfate fluxes here are generally lower than some published data calculated by the same concentration of SO₂ (40 ppb) because the gas- and aqueous-phase parameters in this work were corrected by the experimental temperature (296.8K) rather than the standard temperature (271 K) used previously (Cheng et al., 2016; Gen et al., 2019; Liu et al., 2020; Su et al., 2020; Wang et al., 2020a; Liu et al., 2021a). Considering that part of the relevant parameters were experimentally determined under room temperature with the lack of temperature dependence, uncertainties may exist in the discussions on cold environments. The sulfate formation in this work was assessed near room temperature that is pertinent to the nature of sandstorm occurring during late spring and early summer in East Asia (Wu et al., 2020; Ren et al., 2021). During nighttime, the gas-phase, aqueous-phase and heterogeneous chemistries explain 31.6, 39.8 and 28.6% of the secondary sulfate aerosols, respectively (Fig. 4b). The diurnal contribution proportions of gas-phase chemistry (45.5%) and aqueous-phase chemistry (41.4%) exceed their nocturnal levels, thus lowering the heterogeneous proportion to 13.1% during daytime (Fig. 4f). In other words, although the heterogeneous sulfate production during nighttime is quantitatively lower than that during daytime (see Sect. 3.2), the nocturnal heterogeneous chemistry accounts for the higher proportion of secondary sulfate. In the regime of gas-phase chemistry, OH is the predominant oxidant, followed by Cls, while NO₃ contributes little. In liquid phase, TMI-O₂ and H₂O₂ play crucial roles in the oxidation of SO₂, coinciding to the reported results (Fan et al., 2020; Song et al., 2021). Besides, there are lower contributions attributed to the NO₂ during nighttime, as well as the HOBr, photosensitization, nitrate photolysis during daytime. The heterogeneously formed sulfate is mostly ascribed to the dust-driven chemistry rather than the dust-mediated chemistry. The sulfate formation rates of gas-phase, aqueous-phase and heterogeneous chemistries under solar irradiation are respectively 9.4, 6.8 and 3.0 times greater than the corresponding nocturnal results, indicating that the oxidations in gaseous and liquid media could be more kinetically susceptible to the occurrence of sunlight than those relevant to the gas-solid interface. The sulfate contribution proportions of dust heterogeneous chemistry are comparable with those obtained by the OBM model (30.6% for nighttime and 19.4% for daytime) (Xue et al., 2016), as well

as the revised GEOS-Chem model (20-30%) (Tian et al., 2021) and WRF-CMAQ model (up to 12%) (Wang et al., 2012). While the kinetic uptake coefficients used in the previous studies are generally greater than the present experimental results, more pathways were implemented in the current comparison model, thereby causing the parallel comparison results. By contrast, the AMAR model highlighted the dust's photocatalytic surface that contributes remarkable secondary sulfate (>50%) under the constraint simulation conditions (Yu et al., 2017).

In the regime of dust-mediated heterogeneous chemistry, H_2O_2 is the most efficient oxidant, followed by the nocturnal NO_2 and diurnal hypohalous acids (HOBr, HOCl) responsible for less secondary sulfate (Fig. 4c, g). The dust-driven heterogeneous sulfate formation is mainly attributed to IMt that owns the largest proportion in dust community, followed by NAu and SWy with relatively great heterogeneous performances (Fig. 4d and h). The nocturnal and diurnal secondary sulfate fluxes of the dust-driven chemistry are respectively 5.8 and 1.2 times greater than those of the dust-mediated chemistry. In other words, the heterogeneous sulfate formation is primarily ascribed to the dust surface drivers rather than the surface adsorbed oxidants, as experimentally proved by the laboratory studies concerning the heterogeneous SO_2 oxidation on authentic dusts accelerated by the presence of NO_2 (Park et al., 2017), or O_3 (Park et al., 2017), or H_2O_2 (Huang et al., 2015). The kinetic discrepancy between the dust-mediated and dust-driven chemistries is more significant during nighttime than daytime. In the estimation, H_2O_2 is the predominant dust-mediated oxidant and its concentration becomes lower under weaker solar irradiation. During nighttime, the dust-mediated contribution is thus relatively small by the presence of the relatively low H_2O_2 concentration. When investigating the heterogeneous chemistry on dust particles, particle variables are thus more important than gas variables in elucidating the reaction characteristics and atmospheric implications.

The sulfate formation rates of diverse chemistry modes are summarized as a function of particle acidity as presented in Fig. 5. Relative to the pH-independent gas-phase chemistry, the aqueous-phase oxidation of SO_2 becomes relatively productive under the extremely acidic and near-neutral situations, while fails to support the rapid sulfate formation within the pH range of 4-5 (minimums at 4.85 for nighttime and 4.55 for daytime), which overlaps the acidity range of the weak dust-mediated heterogeneous chemistry. Noticeably, such selected range includes the acidity of the aged natural dust and overlaps that of the common haze aerosols, suggesting that the heterogeneous drivers of dust surface have profound impacts on the secondary sulfate burst in highly polluted environment (Ding et al., 2019; Song et al., 2019). As proved by the atmospheric observation research, secondary sulfate was discovered to accumulate on the dust-dominant super-micron particles collected in the North China Plain, and this pollution on coarse particles dramatically got worse during the evolutionary stages of haze episodes (Xu et al., 2020). In more detail, the significant sulfate formation in the acidic environment is primarily contributed by the TMI- O_2 pathway where the concentrations of TMIs and H^+ keep increasing as the aerosol water becomes more acidic. When $pH > 5.0$, the formation rate of sulfate increases with the elevated pH, in step with the evolution of the concentration of dissolved sulfur species. Within the entire pH range, the aqueous-phase chemistry is more efficient than the dust-mediated heterogeneous chemistry in contributing to secondary sulfate.

Apart from sulfate formation rate, SO_2 lifetime is another index evaluating the atmospheric significance of certain oxidation pathway. Calculations of lifetimes can be useful in estimating how long the SO_2 is likely to remain airborne before it is removed

from the atmosphere (Seinfeld and Pandis, 2016). Under dark condition, IMt causes the shortest SO₂ lifetime, followed by NAu and SWy, with those ascribed to KGa and CCa being much longer. IMt owns the largest mass proportion in dust community and thus causes the shortest lifetime. The relatively great reactivities of NAu and SWy link to the second and third shortest SO₂ lifetimes. On the other hand, the weakest reactivity of KGa leads to the second longest lifetime, and the longest result caused by CCa can be partly interpreted by its lowest S_p. The occurrence of solar irradiation alters the lifetime ranking (IMt<SWy<NAu<KGa<CCa), as influenced by the different photoactivities of the clay minerals. The heterogeneous drivers of natural dust surface are comparable with TMI-O₂ in the loss of SO₂, and both of them function as the most important lifespan influencers in the absence of sunlight (Fig. S9a). During daytime, the natural-dust-driven process is only next to the oxidations induced by OH, TMI-O₂ and H₂O₂ (Fig. S9b). The results of SO₂ lifetime agree well with those of sulfate formation rate (Fig. 4), illustrating that the heterogeneous drivers of dust surface are responsible for altering the concentrations of gas-phase and particulate sulfur species.

In summary, gas- and aqueous-phase chemistries function as the most significant influencers of the diurnal lifespan of SO₂, followed by dust-driven heterogeneous chemistry, while during nighttime these three chemistries present closer impacts (Fig. S10). The atmospheric lifetimes of SO₂ induced by all of the studied oxidation pathways are calculated to be 6.17 days during nighttime and 0.99 days during daytime as presented in Fig. 6. Neglecting the dust heterogeneous chemistry may lengthen the SO₂ lifespans to 10.27 and 1.12 days in the absence and presence of solar irradiation, respectively. Analogously, scientists obtained the shorter lifetime of SO₂ from climate model after considering the heterogeneous reaction occurring on volcanic ash particles (Zhu et al., 2020). Clay minerals are more concentrated in the troposphere than volcanic ash and thus have more significant impacts on the removal of atmospheric SO₂.

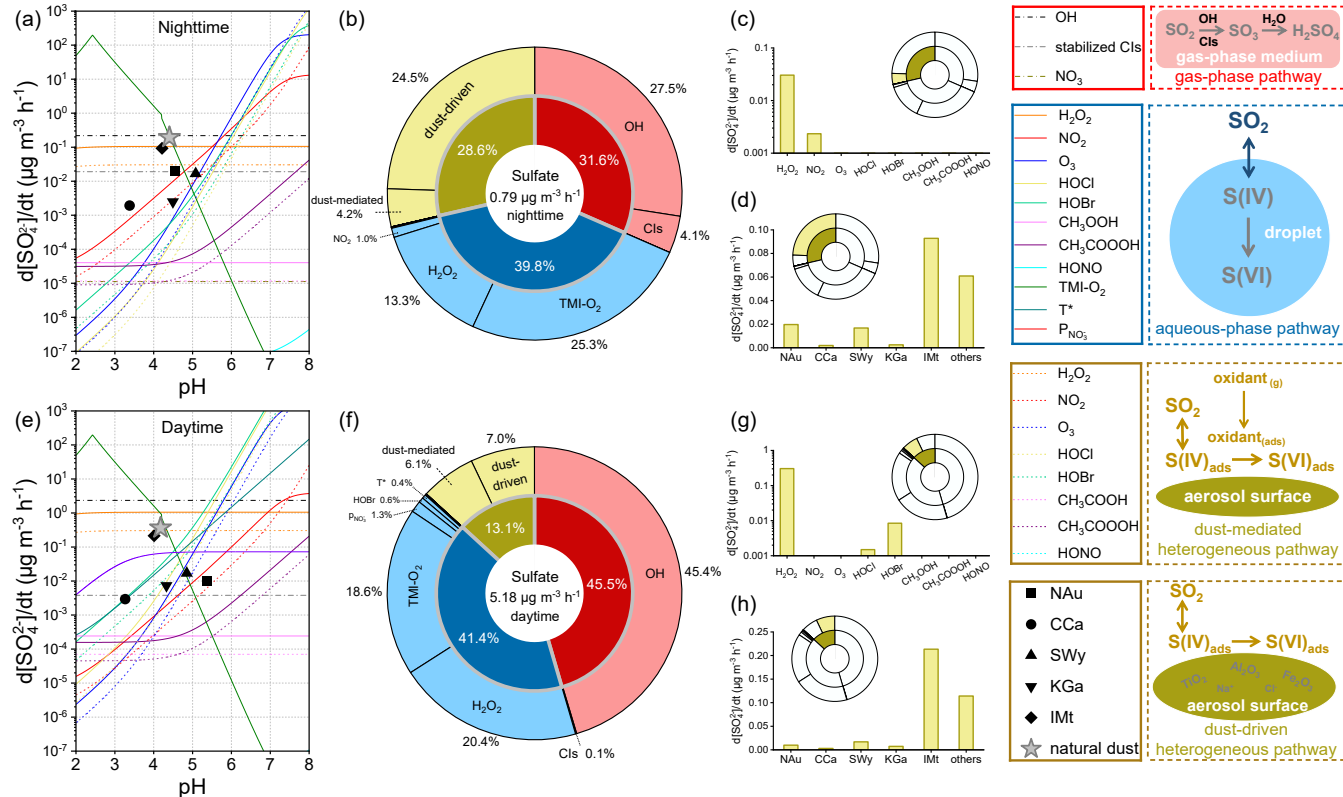


Figure 4. Contributions of diverse oxidation pathways to secondary sulfate aerosols.

Gas-phase chemistry is induced by hydroxyl radical (OH), stabilized Criegee intermediates (CIs), as well as the nitrate radical (NO_3^-) only for nighttime. Aqueous-phase chemistry is induced by hydrogen peroxide (H_2O_2), nitrogen oxide (NO_2), ozone (O_3), hypochlorous acid (HOCl), hypobromous acid (HOBr), methyl hydroperoxide (CH_3OOH), peroxyacetic acid (CH_3COOOH), dissolved nitrous acid (HONO), transition-metal ion-catalyzed oxygen (TMI-O₂), and the photosensitization (T*) and nitrate photolysis ($\text{P}_{\text{NO}_3^-}$) only for daytime. Dust-mediated heterogeneous chemistry is initiated by the surface oxidants co-adsorbed with SO_2 (H_2O_2 , NO_2 , O_3 , HOCl, HOBr, CH_3OOH , CH_3COOOH , HONO). Dust-driven heterogeneous chemistry is ascribed to the heterogeneous drivers (transition-metal-bearing components and water-soluble ions) on the surfaces of natural dust and clay minerals [Nontronite (NAu), Chlorite (CCa), Montmorillonite (SWy), Kaolin (KGa), Illite (IMt)]. The (a-d) nighttime and (e-h) daytime conditions were distinguished by the different parameterizations. (a, e) Particle-acidity-dependent sulfate formation rate of the studied SO_2 oxidation pathways. (b, f) Quantified sulfate contribution proportions of the studied oxidation pathways. Sulfate formation rates of the dust-mediated and dust-driven pathways during (c-d) nighttime and (g-h) daytime. The effects of ionic strength on the aqueous-phase SO_2 oxidation were not taken into account. The dust concentration was set to be $55 \mu\text{g m}^{-3}$ to reflect the common atmospheric condition of China (Zhang et al., 2012). The panels right to the legends illustrate the primary physical-chemical processes of atmospheric sulfate formation. More parameterization and methodology details can be found in the Texts S2-S4 of Supporting Information and Sect. 2.1-2.5 of the main content.

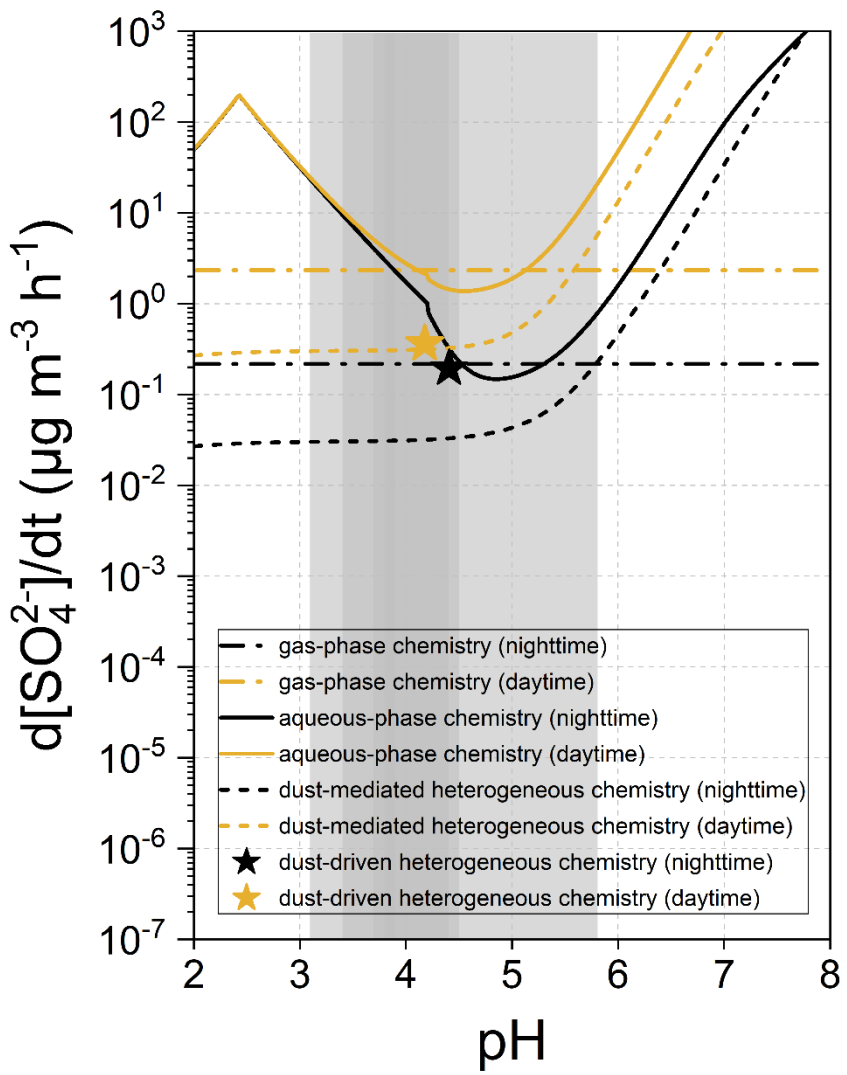


Figure 5. Formation rate of sulfate in the kinetic regimes of gas-phase chemistry, aqueous-phase chemistry and dust heterogeneous chemistry as a function of particle acidity (pH).

495

Grey areas indicate the pH ranges of the polluted particulate matters, with darker ones being more common (Ding et al., 2019).

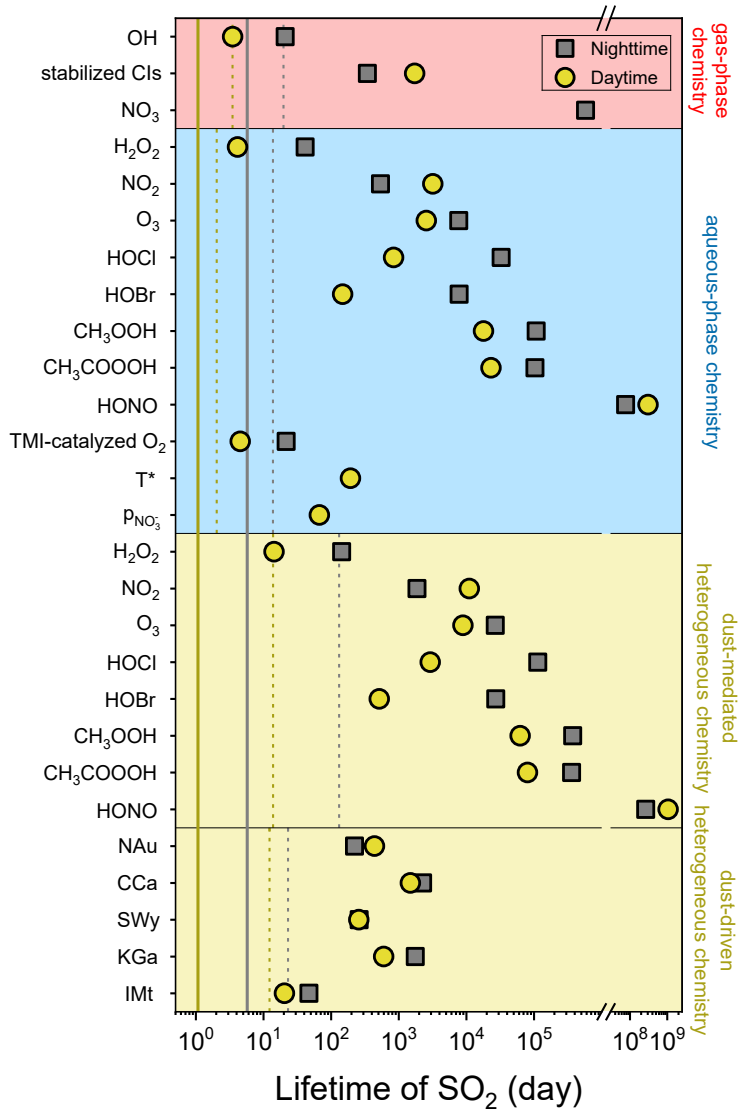


Figure 6. Atmospheric lifetimes of SO_2 induced by the diverse sulfate formation pathways.

Both of the nighttime (grey square) and daytime (yellow circle) conditions were considered. The lifetimes of SO_2 caused by gas-phase, aqueous-phase and dust heterogeneous chemistries are displayed by the dash lines. The atmospheric lifetimes of SO_2 induced by all of the studied oxidation pathways are presented by the solid lines. The effects of ionic strength on the aqueous-phase SO_2 oxidation were not taken into account. The dust concentration was set to be $55 \mu\text{g m}^{-3}$ to reflect the common atmospheric condition of China. More methodology details can be found in Sect. 2.6 of the main content.

3.4 Sensitivity analysis

505 The aforementioned calculations set the concentration of natural dust to be $55 \mu\text{g m}^{-3}$. In contrast to the common atmospheric loading, the burst of sandstorm was normally accompanied by the quickly elevated dust concentration up to thousands of $\mu\text{g m}^{-3}$ (Li et al., 2021; Yin et al., 2021; Filonchyk, 2022). It would be meaningful to estimate the heterogeneous contributions in the dust-rich environments. Theoretically, dust concentration within the ranges of $72\text{--}770 \mu\text{g m}^{-3}$ during nighttime and $24\text{--}260 \mu\text{g m}^{-3}$ during daytime could cause the extra sulfate formation of $0.3\text{--}3.0 \mu\text{g m}^{-3} \text{ h}^{-1}$ (Fig. 7a), in line with the acknowledged range of missing sulfate formation rate (Cheng et al., 2016; Liu et al., 2020), which was found to be positively correlated with PM concentration as well (Cheng et al., 2016). Therefore, the heterogeneous reaction of SO_2 on dust surface is a considerable sulfate formation pathway and may evolve into the missing sulfate source.

510 The occurrence of sandstorm, particularly during nighttime, aggravates the sulfate pollution in coarse aerosol mode (Fig. 7b). For instance, the dust concentration of $200 \mu\text{g m}^{-3}$, which approaches the PM_{10} level in North China on March 2021 (Yin et al., 2021), could heterogeneously explain 44.9% of the secondary sulfate during nighttime, as well as 29.6% during daytime.

515 It is worthwhile to note that, the heterogeneous contribution proportion is susceptible to the evolution of relatively low dust concentration, further increase of dust loading will not significantly elevate the heterogeneous proportion, resulting in a plateau (nighttime) or decrease (daytime) under severe dust pollution. The increased dust concentration facilitates the aqueous-phase TMI-O_2 pathway and the dust-mediated and dust-driven heterogeneous reactions, whereas presents negative impacts on the

520 others by the removal of gaseous oxidants over dust surface. The unsusceptible response to dust concentration, as shown by Fig. 7b, can be related to the increased sulfate contributions from the TMI-O_2 pathway. Unlike the TMI-O_2 pathway and dust-driven chemistry receiving constant positive feedbacks from the increased dust concentration, the dust-mediated chemistry is somewhat affected by the decreased oxidants adsorbed on dust surface. Since the importance of dust-mediated chemistry is more significant during daytime than nighttime, there is a negative correlation between the high dust concentration and 525 heterogeneous contribution proportion under solar irradiation.

The increased dust concentration, in fact, not merely facilitates the heterogeneous chemistry by providing more reactive surfaces, but also affects the gas- and aqueous-phase chemistries by altering the atmospheric abundances of the reactive species therein, as explained below. The evolution of dust pollution from slight to heavy conditions would cause the loss of various gaseous oxidants by heterogeneous uptake, and therefore the gas- and aqueous-phase sulfate fluxes, except that induced by

530 TMI-O_2 , decrease against dust concentration (Bian and Zender, 2003; Tang et al., 2017). Moreover, the dissolution of mineral constituents produces TMIs in aerosol liquid media (Alexander et al., 2009; Shao et al., 2019), and the irradiated mineral dust was reported to emit gaseous ROS by surface photocatalysis (Dupart et al., 2012; Chen et al., 2021). Herein, the studied oxidation pathways are distinguished by their contribution proportions (Fig. 7c and d). The contribution proportions of OH and H_2O_2 decrease against dust loading, while the relative importance of TMI-derived oxidation and dust-driven chemistry 535 become more significant as the dust concentrates. The contribution proportion assigned to dust-mediated chemistry increases with dust concentration at first and then decreases. While the increased dust loading provides more physical space for the

occurrence of dust-mediated reactions, the simultaneously decreased gas-phase oxidants restrain the accumulation of particle-phase oxidants.

Atmospheric lifetime of SO_2 is also affected by the concentration of dust. As shown by Fig. 8a, the lifespan of airborne SO_2 during nighttime is higher than that during daytime, and both of them decrease against dust concentration. Analogous to the heterogeneous contribution proportion (Fig. 7b), the atmospheric lifetime of SO_2 is more susceptible to the variation of dust concentration in clean and slightly polluted environments than heavily polluted conditions. The mild dust pollution, especially its level variations, should be paid more attention. The heterogeneous loss of SO_2 by dust surface was normally evaluated against the gas-phase loss by OH (Ullerstam et al., 2003; Adams et al., 2005; Li et al., 2006; Huang et al., 2015; Ma et al., 2018). Current estimation indicates that the airborne dust with the concentration of $45 \mu\text{g m}^{-3}$ during nighttime, or $91 \mu\text{g m}^{-3}$ during daytime, can be regarded as comparable with OH in controlling the removal of SO_2 (Fig. 8b). Such dust concentrations could be common in the troposphere (Zhang et al., 2012), suggesting that under most atmospheric conditions, the heterogeneous loss of SO_2 by airborne dust surface has a similar magnitude as the main gas-phase loss process and can be taken as an important sink for SO_2 .

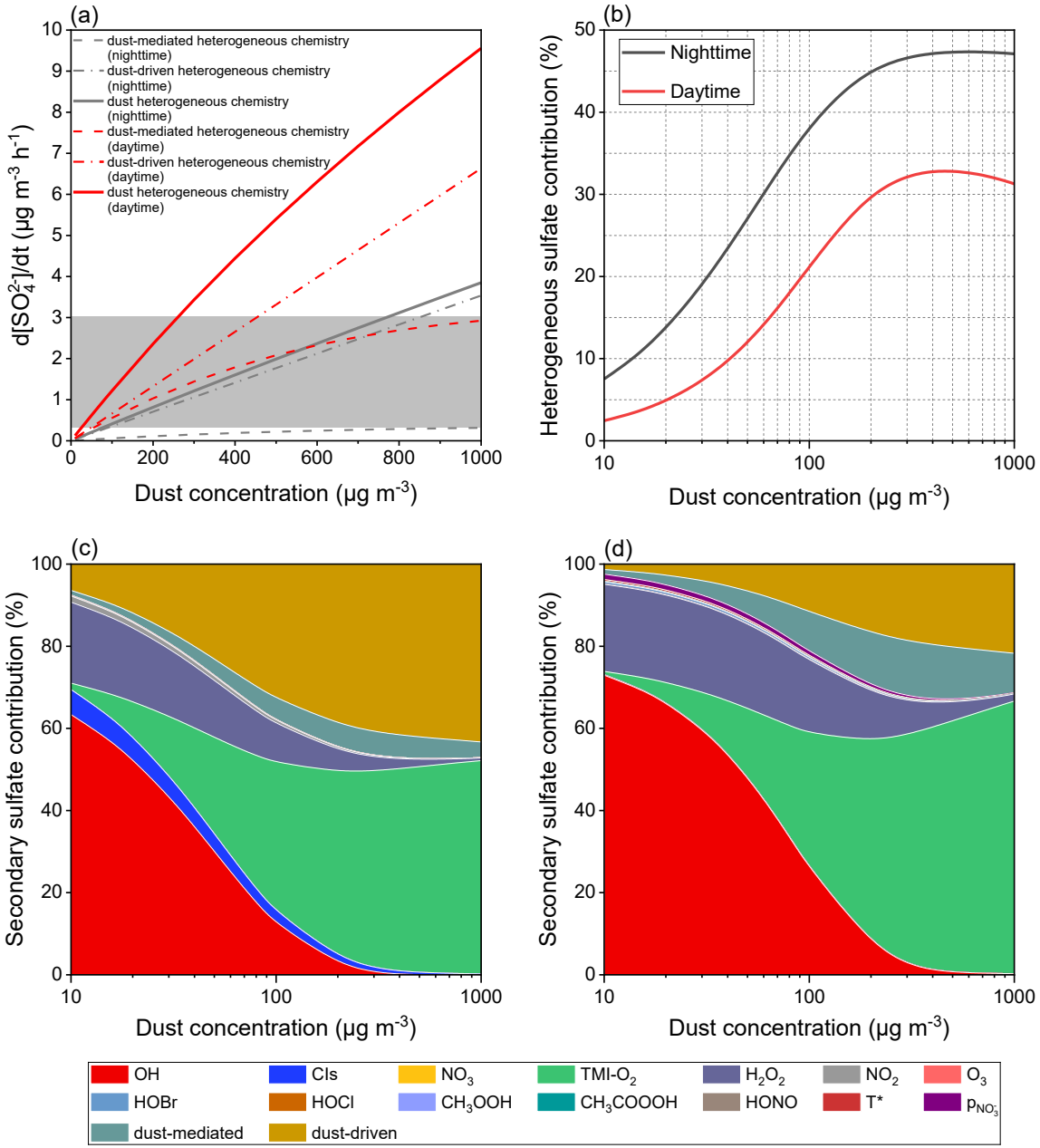


Figure 7. Sensitivity tests of sulfate formation rate on dust concentration.

(a) Sulfate formation rate of diverse dust-related heterogeneous chemistries as a function of dust concentration. The grey area suggests the missing sulfate formation rate ranging from 0.3 to 3 $\mu\text{g m}^{-3} \text{h}^{-1}$ as a reference (Cheng et al., 2016; Liu et al., 2021a).

(b) Heterogeneous sulfate proportion varying with dust concentration. Secondary sulfate contributions attributed to the studied oxidation pathways during (c) nighttime and (d) daytime.

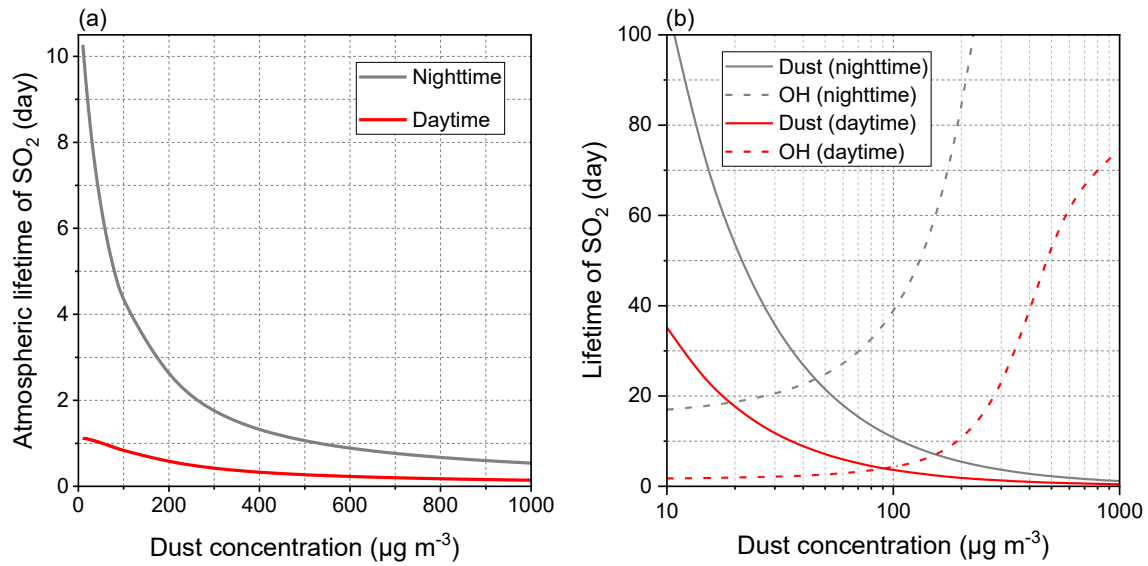


Figure 8. Sensitivity tests of SO_2 lifetime to dust concentration.

(a) Atmospheric lifetime of SO_2 induced by all of the studied pathways varying with dust concentration. (b) Comparison

560

between the SO_2 lifetimes induced by dust heterogeneous chemistry and OH-initiated gas-phase chemistry.

3.5 Uncertainty analysis

The contribution proportion of dust heterogeneous chemistry could be over- or underestimated if considering the uncertainty factors. Herein, the joint impacts of ionic strength (I) and aerosol liquid water content (ALWC) on the aqueous-phase oxidation of SO_2 , as well as the comparison between microdroplet interfacial oxidation and dust-driven heterogeneous chemistry, are 565 additionally discussed to further understand the atmospheric significance of the dust surface drivers under the complex atmospheric conditions.

The aqueous-phase oxidation of SO_2 by H_2O_2 , O_3 , NO_2 and TMI-O_2 was quantified under different I-ALWC parameterizations. At first, the sulfate formation rate was calculated as a function of ionic strength under the studied ALWC of $300 \mu\text{g m}^{-3}$ (Fig. 570 S11). TMI-O_2 and H_2O_2 dominate the liquid oxidation, while the impacts of NO_2 and O_3 only slightly peak at $\sim 1.0 \text{ M}$ in the absence of solar irradiation. Specifically, during nighttime, TMI-O_2 dominates the sulfate formation under the relatively low ionic strength, while the contribution of H_2O_2 exceeds that of TMI-O_2 over the ionic strength of 0.028 M . During daytime, H_2O_2 becomes the dominant oxidant within the studied ionic strength range. Relative to the ionic strength-free calculations, the aqueous oxidation could be weakened by the ionic strength lower than 17.8 M during nighttime or 14.3 M during daytime. Such values can be taken as criteria to distinguish the over- or underestimation of the liquid kinetics under the ALWC of $300 \mu\text{g cm}^{-3}$, which was widely used to characterize the haze events in North China (Cheng et al., 2016).

The joint influences of I and ALWC were further considered (Fig. 8). At each ionic strength, sulfate formation rate associates 575 positively with ALWC. At each ALWC, the increase of ionic strength hinders the aqueous oxidation at first and then facilitates this process, as a consequence resulting in a threshold line distinguishing the negative or positive effects of ionic strength, as presented by Fig. 9a and b. Furthermore, the I-ALWC relationships of California, USA (Stelson and Seinfeld, 1981); Beijing, 580 China (Song et al., 2021); Mexico City, Mexico (Volkamer et al., 2007; Hennigan et al., 2015); and the nine cities of Germany (Scheinhardt et al., 2013) were found to locate left to the thresholds, implying the negative effect of ionic strength under the investigated scenarios (Fig. 9c). Calculated by the reported I-ALWC relationships, the dust-mediated chemistry contributes 4.3%-20.1% of the secondary sulfate during nighttime and 6.8%-22.0% during daytime, and the dust-driven chemistry accounts for respectively 29.1%-41.6% and 9.9%-12.4% of the sulfate formation in the absence and presence of sunlight (Fig. 585 9d). Therefore, the heterogeneous contribution proportions in the complex atmospheric environments can be even higher than those estimated by the present study.

Besides the gas-solid interface, gas-liquid interface is another type of medium that supports the rapid formation of sulfate. The 590 oxidation of SO_2 was found to proceed at the interfacial layer of a droplet with higher kinetics than the bulk process (Jayne and Davidovits, 1990). Recently, the interfacial roles of O_2 (Hung and Hoffmann, 2015; Hung et al., 2018; Chen et al., 2022), NO_2 (Liu and Abbatt, 2021; Yu, 2021) and Mn^{2+} (Zhang et al., 2021; Wang et al., 2021a; Wang et al., 2022c) have been quantitatively investigated. Figure 10 compares dust-driven heterogeneous chemistry with the documented gas-liquid interfacial oxidations. As reported by Hung et al. (2015, 2018), acidic droplet interface favors the noncatalyzed oxidation by the presence of sufficient SO_3^{2-} and SO_4^{2-} when $\text{pH} < 4.0$, which can be further explained by the structure differences of water

595 at the interface versus the characteristic water structure in bulk-phase water. Recently, Chen et al. (2022) reevaluated the sulfate formation by interfacial O₂ within the pH range of 3.5-4.5 and discovered the positive dependence toward ionic strength. The oxidation of SO₂ by interfacial NO₂ was documented to display the similar pH dependence as that occurs in bulk solution. The sulfate contribution of interfacial Mn²⁺ is associated positively with particle acidity. Overall, the O₂ at acidic interface dominates the SO₂ oxidation over pH<4.0, whereas over pH>4.0 the interfacial oxidation is primarily controlled by Mn²⁺.

596 Comparing the sulfate formation rates under the same particle acidity, the dust surface drivers generally present greater 600 reactivity than the interfacial NO₂ and O₂. Under the ionic strength of 40 M, the reactivity of interfacial O₂ can be regarded as equivalent to that of the dust surface drivers during nighttime. Interfacial Mn²⁺ kinetically exceeds the dust surface drivers through kinetic regime. For instance, the Mn²⁺-catalyzed oxidation characterized by Wang et al. (2021a) is respectively 6.5 and 1.7 times more efficient than the dust-driven chemistry in forming sulfate aerosols during nighttime and daytime.

605 It is worthwhile to note that, the dust-driven heterogeneous chemistry was investigated by the infrared technique focusing on the bulk particle sample rather than air-suspended particles. Up to now, the micro-scale effects of dust particle have not been systematically studied. Suspended ATD was concerned in a smog chamber research and its reactivity toward SO₂ was characterized by the net uptake coefficient of 1.71×10^{-6} under dark condition (Park and Jang, 2016). Such kinetic constant is approximately one order of magnitude higher than those obtained from the film-based flow tube experiments ($\sim 1.75 \times 10^{-7}$) under the parallel experimental conditions (Zhang et al., 2019b). Therefore, the dust-driven heterogeneous chemistry in 610 ambient atmosphere may approach the microdroplet interfacial reactivity in the removal of SO₂ and formation of sulfate.

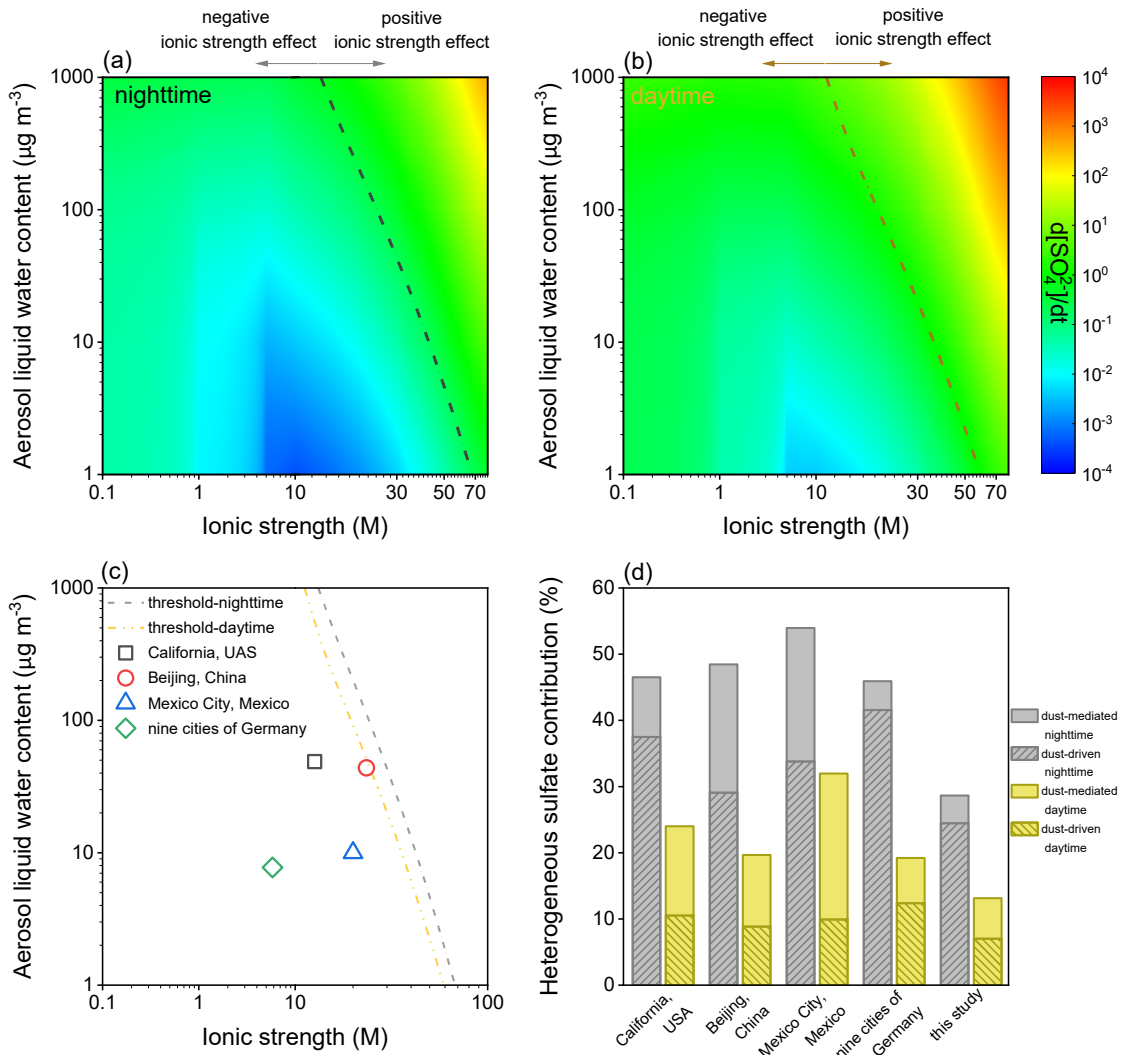


Figure 9. Joint influences of ionic strength (I) and aerosol liquid water content (ALWC) on the aqueous-phase oxidation of SO_2 .

Aqueous-phase sulfate formation rate varying with I and ALWC during (a) nighttime and (b) daytime. The dash-dot lines

615

indicate the thresholds distinguishing the negative or positive effects of ionic strength. (c) Reported I-ALWC relationships versus the nocturnal and diurnal thresholds. The field-observed date were derived from the measurements in California, USA (Stelson and Seinfeld, 1981); Beijing, China (Song et al., 2021); Mexico City, Mexico (Volkamer et al., 2007; Hennigan et al., 2015); and the nine cities of Germany (Scheinhardt et al., 2013). (d) Heterogeneous contribution proportions calculated by the reported I-ALWC relationships and the parameterization of this study (ionic strength-free settings and an ALWC of $300 \mu\text{g m}^{-3}$ for aqueous-phase chemistry; dust concentration of $55 \mu\text{g m}^{-3}$ for heterogeneous chemistry).

620

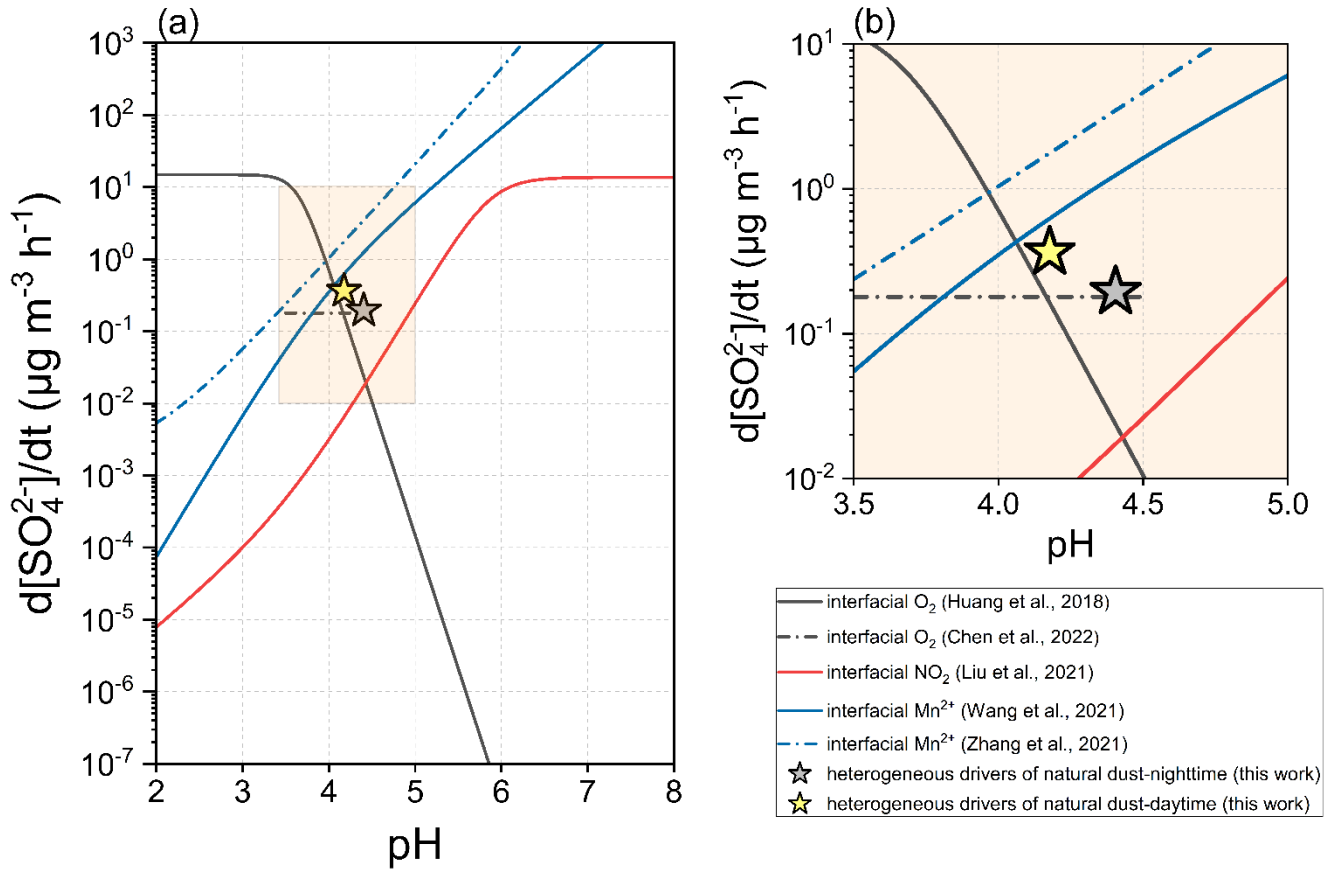


Figure 10. Kinetics comparison between microdroplet interfacial oxidation and dust-driven heterogeneous chemistry.

The interfacial oxidation of SO_2 can be induced by the O_2 , or NO_2 , or Mn^{2+} at aerosol particle interfaces. The O_2 -dominated oxidation can be assessed by the method concluded by Hung et al. (2018). Chen et al. (2022) refreshed the assessment method relevant to the interfacial O_2 , and the result here was obtained under the ionic strength of 40 M. The NO_2 -dominated oxidation was assessed based on the work of Liu and Abbatt (2021). The Mn^{2+} -dominated oxidation can be assessed by the methods from Wang et al. (2021a) and Zhang et al. (2021). More parameterization and methodology details can be found in the Text S5 of Supporting Information.

4 Conclusions and implications

630 This study attempted to deeply understand the importance of heterogeneous chemistry, particularly that induced by the dust surface drivers, in the loss of airborne SO_2 and formation of sulfate aerosols. Based on the correlation and regression analysis, transition metal elements, particularly Fe for dark condition, and Al and Ti for photoreaction, were determined to dominate the heterogeneous oxidation, while water-soluble ions present minor influences. A series of empirical equations were developed to kinetically predict the dust-driven process. The Al, Fe, Ti-bearing mineralogical components, as well as their mixtures, are

635 thus recommended as appropriate proxies for the laboratory research. The reactive uptake coefficients for the dust-driven sulfate formation were calculated to be 6.08×10^{-6} during nighttime and 1.14×10^{-5} during daytime, corresponding respectively to the atmospheric sulfate formation rates of 0.195 and $0.365 \mu\text{g m}^{-3} \text{h}^{-1}$ in the presence of $55 \mu\text{g m}^{-3}$ natural dust.

640 Dust heterogeneous chemistry is suggested to explain 28.6% of the secondary sulfate aerosols during nighttime and 13.1% during daytime, and the dust surface drivers act as the dominate contributors. Moreover, dust heterogeneous chemistry affects the atmospheric lifetime of SO_2 . The increased dust concentration may aggravate the secondary sulfate pollution and has the potential to explain the acknowledged missing sulfate formation rate ($0.3\text{-}3 \mu\text{g m}^{-3} \text{h}^{-1}$). Ionic strength and aerosol liquid water content not merely influence the liquid kinetics, but further affect the assessment of heterogeneous contributions. The heterogeneous contribution proportions estimated by the reported I-ALWC relationships could be even greater than those calculated by this study. Additionally, dust heterogeneous chemistry in the atmosphere is believed to be kinetically comparable

645 with the microdroplet interfacial SO_2 oxidation.

Overall, this study suggests that the implementation of heterogeneous processes into atmospheric models shall vastly improve the agreement between the modeled and observed sulfate concentrations. Dust heterogeneous chemistry should be treated as a significant contributor of secondary aerosols rather than a plausible influencer. More necessarily, the heterogeneous drivers of dust surface are needed to be viewed as an important research focus. Zheng et al. (2015) revised the CMAQ model by adding

650 heterogeneous chemistry mechanism and observed the accurate simulation run upon determining the uptake coefficient to be 2.0×10^{-5} , which is higher than the reactive uptake coefficients of the dust heterogeneous chemistry discussed by this work (7.04×10^{-6} for nighttime and 1.55×10^{-5} for daytime). As a consequence, other solid aerosol surfaces, such as those of sea salts (Laskin et al., 2003; Rossi, 2003) and carbonaceous particles (He and He, 2020; Zhang et al., 2020), would better be taken into the following heterogeneous discussions together with the dust chemistry. In addition, the influence of meteorological factors, like temperature, humidity and irradiance, on the atmospheric relevance of heterogeneous chemistry warrants further research.

655 Heterogeneous laboratory results were scarcely discussed together with other SO_2 conversion routes. This study attempted to set an example for kinetically comparing the heterogeneous process characterized by laboratory work with the widely documented gas- and aqueous-phase data. Relative to the three-dimensional numerical models, the developed comparison model involves more oxidation pathways. Moreover, the aqueous-phase chemistry here is relevant to aerosol particle rather

than cloud/fog droplet, and the parameterization here could be more appropriate for simulating the fine particulate matters that were frequently collected by atmospheric observation campaigns and compared with modeling data. Further, the heterogeneous chemistry was classified into the dust-mediated and dust-driven modes to better distinguish the key surface impactors. Therefore, the dynamic comparison in this study has advantages over the traditional atmospheric chemistry models, and is thus recommended for the following heterogeneous laboratory research to systematically compare the experimental data with the acknowledged gas-phase/aqueous-phase/heterogeneous oxidation pathways.

This work also broadens the application of infrared technique in the atmospheric laboratory research. Apart from measuring the reactive uptake coefficient normally concerned, this study moved forward to bridge the relationship between particle acidity and sulfate formation rate by analyzing the shape and intensity of infrared spectrum, and further compared the dust heterogeneous chemistry with other sulfate formation pathways. This research not merely provides a promising methodology for the future heterogeneous research utilizing the classic *in-situ* DRIFTS approach, but also helps to take good advantages of the infrared technique in the laboratory studies in relation to atmospheric heterogeneous chemistry.

Data availability. The data that support the results are available from the corresponding author upon request.

Author Contributions. T.W. designed the experiments and processed the data, and wrote the paper together with Y.L; H.C. and Z.W. measured the physical and chemical properties of the particle samples; H.F., J.C., and L.Z. provided guidance in the data analysis and paper writing.

Competing interests. The authors declare no competing financial interest.

Financial support. The research was financially supported by National Natural Science Foundation of China (No. 22176036, 21976030, 22006020) and Natural Science Foundation of Shanghai (No. 19ZR1471200).

References

685 Abou-Ghanem, M., Oliynyk, A. O., Chen, Z., Matchett, L. C., McGrath, D. T., Katz, M. J., Locock, A. J., and Styler, S. A.: Significant Variability in the Photocatalytic Activity of Natural Titanium-Containing Minerals: Implications for Understanding and Predicting Atmospheric Mineral Dust Photochemistry, *Environ. Sci. Technol.*, 54, 13509-13516, <http://doi.org/10.1021/acs.est.0c05861>, 2020.

690 Adams, J. W., Rodriguez, D., and Cox, R. A.: The uptake of SO₂ on Saharan dust: a flow tube study, *Atmos. Chem. Phys.*, 5, 2679-2689, <http://doi.org/10.5194/acpd-5-2643-2005>, 2005.

695 Alexander, B., Allman, D. J., Amos, H. M., Fairlie, T. D., Dachs, J., Hegg, D. A., and Sletten, R. S.: Isotopic constraints on the formation pathways of sulfate aerosol in the marine boundary layer of the subtropical northeast Atlantic Ocean, *J. Geophys. Res.: Atmos.*, 117, D6304, <http://doi.org/10.1029/2011JD016773>, 2012.

700 Alexander, B., Park, R. J., Jacob, D. J., and Gong, S.: Transition metal-catalyzed oxidation of atmospheric sulfur: Global implications for the sulfur budget, *J. Geophys. Res.*, 114, D2309, <http://doi.org/10.1029/2008JD010486>, 2009.

705 Antoniou, M. G., Boraei, I., Solakidou, M., Deligiannakis, Y., Abhishek, M., Lawton, L. A., and Edwards, C.: Enhancing photocatalytic degradation of the cyanotoxin microcystin-LR with the addition of sulfate-radical generating oxidants, *J. Hazard. Mater.*, 360, 461-470, <http://doi.org/10.1016/j.jhazmat.2018.07.111>, 2018.

710 Ault, A. P.: Aerosol Acidity: Novel Measurements and Implications for Atmospheric Chemistry, *Accounts Chem. Res.*, 53, 1703-1714, <http://doi.org/10.1021/acs.accounts.0c00303>, 2020.

715 Baltrusaitis, J., Jayaweera, P. M., and Grassian, V. H.: Sulfur Dioxide Adsorption on TiO₂ Nanoparticles: Influence of Particle Size, Coadsorbates, Sample Pretreatment, and Light on Surface Speciation and Surface Coverage, *J. Phys. Chem. C*, 115, 492-500, <http://doi.org/10.1021/jp108759b>, 2010.

720 Berglen, T. F., Berntsen, T. K., Isaksen, I. S. A., and Sundet, J. K.: A global model of the coupled sulfur/oxidant chemistry in the troposphere: The sulfur cycle, *J. Geophys. Res.*, 109, D19310, <http://doi.org/10.1029/2003JD003948>, 2004.

725 Bian, H., and Zender, C. S.: Mineral dust and global tropospheric chemistry: Relative roles of photolysis and heterogeneous uptake, *J. Geophys. Res.: Atmos.*, 108, 4672, <http://doi.org/10.1029/2002JD003143>, 2003.

730 Chen, H., Nanayakkara, C. E., and Grassian, V. H.: Titanium dioxide photocatalysis in atmospheric chemistry, *Chem. Rev.*, 112, 5919-5948, <http://doi.org/10.1021/cr3002092>, 2012.

735 Chen, Q., Schmidt, J. A., Shah, V., Jaeglé, L., Sherwen, T., and Alexander, B.: Sulfate production by reactive bromine: Implications for the global sulfur and reactive bromine budgets, *Geophys. Res. Lett.*, 44, 7069-7078, <http://doi.org/10.1002/2017GL073812>, 2017.

740 Chen, Y., Tong, S., Li, W., Liu, Y., Tan, F., Ge, M., Xie, X., and Sun, J.: Photocatalytic Oxidation of SO₂ by TiO₂: Aerosol Formation and the Key Role of Gaseous Reactive Oxygen Species, *Environ. Sci. Technol.*, 55, 9784-9793, <http://doi.org/10.1021/acs.est.1c01608>, 2021.

745 Chen, Z., Liu, P., Wang, W., Cao, X., Liu, Y., Zhang, Y., and Ge, M.: Rapid Sulfate Formation via Uncatalyzed Autoxidation of Sulfur Dioxide in Aerosol Microdroplets, *Environ. Sci. Technol.*, 56, 7637-7646, <http://doi.org/10.1021/acs.est.2c00112>, 2022.

750 Cheng, Y., Zheng, G., Wei, C., Mu, Q., Zheng, B., Wang, Z., Gao, M., Zhang, Q., He, K., Carmichael, G., Pöschl, U., and Su, H.: Reactive nitrogen chemistry in aerosol water as a source of sulfate during haze events in China, *Sci. Adv.*, 2, e1601530, <http://doi.org/10.1126/sciadv.1601530>, 2016.

755 Chu, B., Wang, Y., Yang, W., Ma, J., Ma, Q., Zhang, P., Liu, Y., and He, H.: Effects of NO₂ and C₃H₆ on the heterogeneous oxidation of SO₂ on TiO₂ in the presence or absence of UV-Vis irradiation, *Atmos. Chem. Phys.*, 19, 14777-14790, <http://doi.org/10.5194/acp-19-14777-2019>, 2019.

760 Chughtai, A. R., Brooks, M. E., and Smith, D. M.: Effect of metal oxides and black carbon (soot) on SO₂/O₂/H₂O reaction systems, *Aerosol Sci. Tech.*, 19, 121-132, <http://doi.org/10.1080/02786829308959626>, 1993.

765 Clegg, M., and Abbatt, D.: Uptake of Gas-Phase SO₂ and H₂O₂ by Ice Surfaces: Dependence on Partial Pressure, Temperature, and Surface Acidity, *J. Phys. Chem. A*, 105, 6630-6636, <http://doi.org/10.1021/jp010062r>, 2001a.

770 Clegg, S. M., and Abbatt, J. P. D.: Oxidation of SO₂ by H₂O₂ on ice surfaces at 228 K: a sink for SO₂ in ice clouds, *Atmos.*

Chem. Phys., 1, 73-78, <http://doi.org/10.5194/acp-1-73-2001, 2001b>.

730 Darif, B., Ojala, S., Pirault-Roy, L., Bensitel, M., Brahmi, R., and Keiski, R. L.: Study on the catalytic oxidation of DMDS over Pt-Cu catalysts supported on Al_2O_3 , AlSi_{20} and SiO_2 , Appl. Catal., B, 181, 24-33, <http://doi.org/10.1016/j.apcatb.2015.07.050, 2016>.

735 Ding, J., Zhao, P., Su, J., Dong, Q., Du, X., and Zhang, Y.: Aerosol pH and its driving factors in Beijing, Atmos. Chem. Phys., 19, 7939-7954, <http://doi.org/10.5194/acp-19-7939-2019, 2019>.

Du, C., Kong, L., Zhanzakova, A., Tong, S., Yang, X., Wang, L., Fu, H., Cheng, T., Chen, J., and Zhang, S.: Impact of adsorbed nitrate on the heterogeneous conversion of SO_2 on $\alpha\text{-Fe}_2\text{O}_3$ in the absence and presence of simulated solar irradiation, Sci. Total Environ., 649, 1393-1402, <http://doi.org/10.1016/j.scitotenv.2018.08.295, 2019>.

Dupart, Y., King, S. M., Nekat, B., Nowak, A., Wiedensohler, A., Herrmann, H., David, G., Thomas, B., Miffre, A., Rairoux, P., Anna, B. D., and George, C.: Mineral dust photochemistry induces nucleation events in the presence of SO_2 , Proc. Natl. Acad. Sci. U. S. A., 109, 20842-20847, <http://doi.org/10.1073/pnas.1212297109, 2012>.

740 Fairlie, T. D., Jacob, D. J., Dibb, J. E., Alexander, B., Avery, M. A., van Donkelaar, A., and Zhang, L.: Impact of mineral dust on nitrate, sulfate, and ozone in transpacific Asian pollution plumes, Atmos. Chem. Phys., 10, 3999-4012, <http://doi.org/10.5194/acp-10-3999-2010, 2010>.

745 Fan, M., Zhang, Y., Lin, Y., Li, J., Cheng, H., An, N., Sun, Y., Qiu, Y., Cao, F., and Fu, P.: Roles of Sulfur Oxidation Pathways in the Variability in Stable Sulfur Isotopic Composition of Sulfate Aerosols at an Urban Site in Beijing, China, Environ. Sci. Technol. Lett., 7, 883-888, <http://doi.org/10.1021/acs.estlett.0c00623, 2020>.

Filonchyk, M.: Characteristics of the severe March 2021 Gobi Desert dust storm and its impact on air pollution in China, Chemosphere, 287, 132219, <http://doi.org/10.1016/j.chemosphere.2021.132219, 2022>.

Fu, H., Cwiertny, D. M., Carmichael, G. R., Scherer, M. M., and Grassian, V. H.: Photoreductive dissolution of Fe-containing mineral dust particles in acidic media, J. Geophys. Res., 115, D11304, <http://doi.org/10.1029/2009JD012702, 2010>.

750 Fu, H., Xu, T., Yang, S., Zhang, S., and Chen, J.: Photoinduced formation of Fe(III)-sulfato complexes on the surface of $\alpha\text{-Fe}_2\text{O}_3$ and their photochemical performance, J. Phys. Chem. C, 113, 11316-11322, <http://doi.org/10.1021/jp8088275, 2009>.

Gen, M., Zhang, R., Huang, D., Li, Y., and Chan, C. K.: Heterogeneous Oxidation of SO_2 in Sulfate Production during Nitrate Photolysis at 300 nm: Effect of pH, Relative Humidity, Irradiation Intensity, and the Presence of Organic Compounds, Environ. Sci. Technol., 53, 8757-8766, <http://doi.org/10.1021/acs.est.9b01623, 2019>.

755 Goodman, A. L., Li, P., Usher, C. R., and Grassian, V. H.: Heterogeneous uptake of sulfur dioxide on aluminum and magnesium oxide particles, J. Phys. Chem. A, 105, 6109-6120, <http://doi.org/10.1021/jp04423z, 2001>.

Guan, C., Li, X., Luo, Y., and Huang, Z.: Heterogeneous Reaction of NO_2 on $\alpha\text{-Al}_2\text{O}_3$ in the Dark and Simulated Sunlight, J. Phys. Chem. A, 118, 6999-7006, <http://doi.org/10.1021/jp503017k, 2014>.

760 Han, L., Liu, X., Chen, Y., Xiang, X., Cheng, S., and Wang, H.: Key factors influencing the formation of sulfate aerosol on the surface of mineral aerosols: Insights from laboratory simulations and ACSM measurements, Atmos. Environ., 253, 118341, <http://doi.org/10.1016/j.atmosenv.2021.118341, 2021>.

Hanson, D. R., Ravishankara, A. R., and Solomon, S.: Heterogeneous reactions in sulfuric acid aerosols: A framework for model calculations, J. Geophys. Res.: Atmos., 99, 3615-3629, <http://doi.org/10.1029/93JD02932, 1994>.

765 Harris, E., Sinha, B., Foley, S., Crowley, J. N., Borrmann, S., and Hoppe, P.: Sulfur isotope fractionation during heterogeneous oxidation of SO_2 on mineral dust, Atmos. Chem. Phys., 12, 4867-4884, <http://doi.org/10.5194/acp-12-4867-2012, 2012>.

Haynes, W. M.: Handbook of Chemistry and Physics, CRC Press, New York, 2014.

He, G., and He, H.: Water Promotes the Oxidation of SO_2 by O_2 over Carbonaceous Aerosols, Environ. Sci. Technol., 54, 7070-7077, <http://doi.org/10.1021/acs.est.0c00021, 2020>.

770 He, H., Wang, Y., Ma, Q., Ma, J., Chu, B., Ji, D., Tang, G., Liu, C., Zhang, H., and Hao, J.: Mineral dust and NO_x promote the conversion of SO_2 to sulfate in heavy pollution days, Sci. Rep.-UK, 4, 4172, <http://doi.org/10.1038/srep04172, 2014>.

He, P., Alexander, B., Geng, L., Chi, X., Fan, S., Zhan, H., Kang, H., Zheng, G., Cheng, Y., Su, H., Liu, C., and Xie, Z.: Isotopic constraints on heterogeneous sulfate production in Beijing haze, Atmos. Chem. Phys., 18, 5515-5528, <http://doi.org/10.5194/acp-18-5515-2018, 2018>.

775 He, X., and Zhang, Y.: Influence of relative humidity on SO_2 oxidation by O_3 and NO_2 on the surface of TiO_2 particles: Potential for formation of secondary sulfate aerosol, Spectrochim. Acta, Part A, 219, 121-128, <http://doi.org/10.1016/j.saa.2019.04.046, 2019>.

Hennigan, C. J., Izumi, J., Sullivan, A. P., Weber, R. J., and Nenes, A.: A critical evaluation of proxy methods used to estimate

the acidity of atmospheric particles, *Atmos. Chem. Phys.*, 15, 2775-2790, <http://doi.org/10.5194/acp-15-2775-2015>, 2015.

780 Himmelblau, D. M.: Diffusion of dissolved gases in liquids, *Chem. Rev.*, 64, 527-550, <http://doi.org/10.1021/cr60231a002>, 1964.

Huang, L., An, J., Koo, B., Yarwood, G., Yan, R., Wang, Y., Huang, C., and Li, L.: Enhanced sulfate formation through SO_2+NO_2 heterogeneous reactions during heavy winter haze in the Yangtze River Delta region, China, *Atmos. Chem. Phys.*, 19, 14311-14328, <http://doi.org/10.5194/acp-2019-292>, 2019.

785 Huang, L., Zhao, Y., Li, H., and Chen, Z.: Kinetics of heterogeneous reaction of sulfur dioxide on authentic mineral dust: effects of relative humidity and hydrogen peroxide, *Environ. Sci. Technol.*, 49, 10797-10805, <http://doi.org/10.1021/acs.est.5b03930>, 2015.

Huang, L., Zhao, Y., Li, H., and Chen, Z.: Hydrogen peroxide maintains the heterogeneous reaction of sulfur dioxide on mineral dust proxy particles, *Atmos. Environ.*, 141, 552-559, <http://doi.org/10.1016/j.atmosenv.2016.07.035>, 2016.

790 Huang, Z., Zhang, Z., Kong, W., Feng, S., Qiu, Y., Tang, S., Xia, C., Ma, L., Luo, M., and Xu, D.: Synergistic effect among Cl_2 , SO_2 and NO_2 in their heterogeneous reactions on gamma-alumina, *Atmos. Environ.*, 166, 403-411, <http://doi.org/10.1016/j.atmosenv.2017.06.041>, 2017.

Hung, H., Hsu, M., and Hoffmann, M. R.: Quantification of SO_2 Oxidation on Interfacial Surfaces of Acidic Micro-Droplets: Implication for Ambient Sulfate Formation, *Environ. Sci. Technol.*, 52, 9079-9086, <http://doi.org/10.1021/acs.est.8b01391>, 2018.

795 Hung, H., and Hoffmann, M. R.: Oxidation of Gas-Phase SO_2 on the Surfaces of Acidic Microdroplets: Implications for Sulfate and Sulfate Radical Anion Formation in the Atmospheric Liquid Phase, *Environ. Sci. Technol.*, 49, 13768-13776, <http://doi.org/10.1021/acs.est.5b01658>, 2015.

Jacob, D. J.: Heterogeneous chemistry and tropospheric ozone, *Atmos. Environ.*, 34, 2131-2159, [http://doi.org/10.1016/S1352-2310\(99\)00462-8](http://doi.org/10.1016/S1352-2310(99)00462-8), 2000.

800 Jayne, J. T., and Davidovits, P.: Uptake of $\text{SO}_2(\text{g})$ by Aqueous Surfaces as a Function of pH: The Effect of Chemical Reaction at the Interface, *J. Phys. Chem.*, 94, 6041-6048, <http://doi.org/10.1021/j100378a076>, 1990.

Kim, J., Choe, Y. J., Kim, S. H., and Jeong, K.: Enhancing the decomposition of refractory contaminants on SO_4^{2-} -functionalized iron oxide to accommodate surface $\text{SO}_4^{\cdot-}$ -generated via radical transfer from $\cdot\text{OH}$, *Appl. Catal., B*, 252, 62-76, <http://doi.org/10.1016/j.apcatb.2019.04.015>, 2019.

805 Kong, L. D., Zhao, X., Sun, Z. Y., Yang, Y. W., Fu, H. B., Zhang, S. C., Cheng, T. T., Yang, X., Wang, L., and Chen, J. M.: The effect of nitrate on the heterogeneous uptake of sulfur dioxide on hematite, *Atmos. Chem. Phys.*, 14, 9451-9467, <http://doi.org/10.5194/acp-14-9451-2014>, 2014.

Laskin, A., Gaspar, D. J., Wang, W., Hunt, S. W., Cowin, J. P., Colson, S. D., and Finlayson-Pitts, B. J.: Reactions at Interfaces as a Source of Sulfate Formation in Sea-Salt Particles, *Science*, 301, 340-344, <http://doi.org/10.1126/science.1085374>, 2003.

810 Li, G., Bei, N., Cao, J., Huang, R., and Wu, J.: A possible pathway for rapid growth of sulfate during haze days in China, *Atmos. Chem. Phys.*, 17, 3301-3316, <http://doi.org/10.5194/acp-17-3301-2017>, 2017.

Li, G., Lu, D., Yang, X., Zhang, H., Guo, Y., Qu, G., Wang, P., Chen, L., Ruan, T., Hou, X., Jin, X., Zhang, R., Tan, Q., Zhai, S., Ma, Y., Yang, R., Fu, J., Shi, J., Liu, G., Wang, Q., Liang, Y., Zhang, Q., Liu, Q., and Jiang, G.: Resurgence of Sandstorms Complicates China's Air Pollution Situation, *Environ. Sci. Technol.*, 55, 11467-11469, <http://doi.org/10.1021/acs.est.1c03724>, 2021.

815 Li, J., Shang, J., and Zhu, T.: Heterogeneous reactions of SO_2 on ZnO particle surfaces, *Sci. China: Chem.*, 54, 161-166, <http://doi.org/10.1007/s11426-010-4167-9>, 2010.

Li, J., Zhang, Y., Cao, F., Zhang, W., Fan, M., Lee, X., and Michalski, G.: Stable Sulfur Isotopes Revealed a Major Role of Transition-Metal Ion-Catalyzed SO_2 Oxidation in Haze Episodes, *Environ. Sci. Technol.*, 54, 2626-2634, <http://doi.org/10.1021/acs.est.9b07150>, 2020a.

820 Li, K., Kong, L., Zhanzakova, A., Tong, S., Shen, J., Wang, T., Chen, L., Li, Q., Fu, H., and Zhang, L.: Heterogeneous Conversion of SO_2 on Nano $\alpha\text{-Fe}_2\text{O}_3$: the Effect of Morphology, Light Illumination and Relative Humidity, *Environ. Sci.: Nano*, 6, 1838-1851, <http://doi.org/10.1039/C9EN00097F>, 2019.

Li, L., Chen, Z. M., Zhang, Y. H., Zhu, T., Li, J. L., and Ding, J.: Kinetics and mechanism of heterogeneous oxidation of sulfur dioxide by ozone on surface of calcium carbonate, *Atmos. Chem. Phys.*, 6, 2453-2464, <http://doi.org/10.5194/acp-6-2453-2006>, 2006.

825 Li, L., Chen, Z. M., Zhang, Y. H., Zhu, T., Li, S., Li, H. J., Zhu, L. H., and Xu, B. Y.: Heterogeneous oxidation of sulfur

dioxide by ozone on the surface of sodium chloride and its mixtures with other components, *J. Geophys. Res.*, 112, D18301, <http://doi.org/10.1029/2006JD008207>, 2007.

830 Li, T., Wang, X., Chen, Y., Liang, J., and Zhou, L.: Producing ·OH, SO₄^{·-} and ·O₂^{·-} in heterogeneous Fenton reaction induced by Fe₃O₄-modified schwertmannite, *Chem. Eng. J.*, 393, 124735, <http://doi.org/10.1016/j.cej.2020.124735>, 2020b.

835 Li, S., Zhang, F., Jin, X., Sun, Y., Wu, H., Xie, C., Chen, L., Liu, J., Wu, T., Jiang, S., Cribb, M., and Li, Z.: Characterizing the ratio of nitrate to sulfate in ambient fine particles of urban Beijing during 2018-2019, *Atmos. Environ.*, 237, 117662, <http://doi.org/10.1016/j.atmosenv.2020.117662>, 2020c.

840 Liu, C., Ma, Q., Liu, Y., Ma, J., and He, H.: Synergistic reaction between SO₂ and NO₂ on mineral oxides: a potential formation pathway of sulfate aerosol, *Phys. Chem. Chem. Phys.*, 14, 1668-1676, <http://doi.org/10.1039/C1CP22217A>, 2012.

845 Liu, J., Wu, D., Fan, S., Mao, X., and Chen, H.: A one-year, on-line, multi-site observational study on water-soluble inorganic ions in PM_{2.5} over the Pearl River Delta region, China, *Sci. Total Environ.*, 601-602, 1720-1732, <http://doi.org/10.1016/j.scitotenv.2017.06.039>, 2017c.

850 Liu, T., Chan, A. W. H., and Abbatt, J. P. D.: Multiphase Oxidation of Sulfur Dioxide in Aerosol Particles: Implications for Sulfate Formation in Polluted Environments, *Environ. Sci. Technol.*, 55, 4227-4242, <http://doi.org/10.1021/acs.est.0c06496>, 2021a.

Liu, T., Clegg, S. L., and Abbatt, J. P. D.: Fast oxidation of sulfur dioxide by hydrogen peroxide in deliquesced aerosol particles, *Proc. Natl. Acad. Sci. U. S. A.*, 117, 1354-1359, <http://doi.org/10.1073/pnas.1916401117>, 2020.

855 Liu, T., and Abbatt, J. P. D.: Oxidation of sulfur dioxide by nitrogen dioxide accelerated at the interface of deliquesced aerosol particles, *Nat. Chem.*, 13, 1173-1177, <http://doi.org/10.1038/s41557-021-00777-0>, 2021.

Liu, W., He, X., Pang, S., and Zhang, Y.: Effect of relative humidity on O₃ and NO₂ oxidation of SO₂ on α -Al₂O₃ particles, *Atmos. Environ.*, 167, 245-253, <http://doi.org/10.1016/j.atmosenv.2017.08.028>, 2017b.

860 Liu, X., Chen, W., and Jiang, H.: Facile synthesis of Ag/Ag₃PO₄/AMB composite with improved photocatalytic performance, *Chem. Eng. J.*, 308, 889-896, <http://doi.org/10.1016/j.cej.2016.09.125>, 2017a.

Liu, Y., Feng, Z., Zheng, F., Bao, X., Liu, P., Ge, Y., Zhao, Y., Jiang, T., Liao, Y., Zhang, Y., Fan, X., Yan, C., Chu, B., Wang, Y., Du, W., Cai, J., Bianchi, F., Petäjä, T., Mu, Y., He, H., and Kulmala, M.: Ammonium nitrate promotes sulfate formation through uptake kinetic regime, *Atmos. Chem. Phys.*, 21, 13269-13286, <http://doi.org/10.5194/acp-21-13269-2021>, 2021b.

865 Ma, Q., Liu, Y., Liu, C., Ma, J., and He, H.: A case study of Asian dust storm particles: Chemical composition, reactivity to SO₂ and hygroscopic properties, *J. Environ. Sci.*, 24, 62-71, [http://doi.org/10.1016/S1001-0742\(11\)60729-8](http://doi.org/10.1016/S1001-0742(11)60729-8), 2012.

Ma, Q., Liu, Y., and He, H.: Synergistic effect between NO₂ and SO₂ in their adsorption and reaction on γ -Alumina, *J. Phys. Chem. A*, 112, 6630-6635, <http://doi.org/10.1021/jp802025z>, 2008.

870 Ma, Q., Wang, L., Chu, B., Ma, J., and He, H.: Contrary Role of H₂O and O₂ in the Kinetics of Heterogeneous Photochemical Reactions of SO₂ on TiO₂, *J. Phys. Chem. A*, 123, 1311-1318, <http://doi.org/10.1021/acs.jpca.8b11433>, 2018.

875 Ma, Q., Wang, T., Liu, C., He, H., Wang, Z., Wang, W., and Liang, Y.: SO₂ initiates the efficient conversion of NO₂ to HONO on MgO surface, *Environ. Sci. Technol.*, 51, 3767-3775, <http://doi.org/10.1021/acs.est.6b05724>, 2017.

Martin, M. A., Childers, J. W., and Palmer, R. A.: Fourier transform infrared photoacoustic spectroscopy characterization of sulfur-oxygen species resulting from the reaction of SO₂ with CaO and CaCO₃, *Appl. Spectrosc.*, 41, 120-126, <http://doi.org/10.1366/0003702874868151>, 1987.

880 Maters, E. C., Delmelle, P., Rossi, M. J., and Ayris, P. M.: Reactive Uptake of Sulfur Dioxide and Ozone on Volcanic Glass and Ash at Ambient Temperature, *J. Geophys. Res.: Atmos.*, 122, 10077-10088, <http://doi.org/10.1002/2017JD026993>, 2017.

Mauldin III, R. L., Berndt, T., Sipilä, M., Paasonen, P., Petäjä, T., Kim, S., Kurtén, T., Stratmann, F., Kerminen, V. M., and Kulmala, M.: A new atmospherically relevant oxidant of sulphur dioxide, *Nature*, 488, 193-196, <http://doi.org/10.1038/nature11278>, 2012.

885 Nanayakkara, C. E., Larish, W. A., and Grassian, V. H.: Titanium dioxide nanoparticle surface reactivity with atmospheric gases, CO₂, SO₂, and NO₂: roles of surface hydroxyl groups and adsorbed water in the formation and stability of adsorbed products, *J. Phys. Chem. C*, 118, 23011-23021, <http://doi.org/10.1021/jp504402z>, 2014.

Nanayakkara, C. E., Pettibone, J., and Grassian, V. H.: Sulfur dioxide adsorption and photooxidation on isotopically-labeled titanium dioxide nanoparticle surfaces: roles of surface hydroxyl groups and adsorbed water in the formation and stability of adsorbed sulfite and sulfate, *Phys. Chem. Chem. Phys.*, 14, 6957-6966, <http://doi.org/10.1039/c2cp23684b>, 2012.

890 Ndour, M., Nicolas, M., D Anna, B., Ka, O., and George, C.: Photoreactivity of NO₂ on mineral dusts originating from different

locations of the Sahara desert, *Phys. Chem. Chem. Phys.*, 11, 1312-1319, <http://doi.org/10.1039/b806441e>, 2009.

880 Park, J., Ivanov, A. V., and Molina, M. J.: Effect of Relative Humidity on OH Uptake by Surfaces of Atmospheric Importance, *J. Phys. Chem. A*, 112, 6968-6977, <http://doi.org/10.1021/jp8012317>, 2008.

Park, J., Jang, M., and Yu, Z.: Heterogeneous Photo-oxidation of SO₂ in the Presence of Two Different Mineral Dust Particles: Gobi and Arizona Dust, *Environ. Sci. Technol.*, 51, 9605-9613, <http://doi.org/10.1021/acs.est.7b00588>, 2017.

885 Park, J., and Jang, M.: Heterogeneous photooxidation of sulfur dioxide in the presence of airborne mineral dust particles, *RSC Adv.*, 6, 58617-58627, <http://doi.org/10.1039/C6RA09601H>, 2016.

Peak, D., Ford, R. G., and Sparks, D. L.: An in situ ATR-FTIR investigation of sulfate bonding mechanisms on Goethite., *J. Colloid Interf. Sci.*, 218, 289-299, <http://doi.org/10.1006/jcis.1999.6405>, 1999.

Persson, P., and Vgren, L. L.: Potentiometric and spectroscopic studies of sulfate complexation at the goethite-water interface, *Geochim. Cosmochim. Ac.*, 60, 2789-2799, [http://doi.org/10.1016/0016-7037\(96\)00124-X](http://doi.org/10.1016/0016-7037(96)00124-X), 1996.

890 Pye, H. O. T., Nenes, A., Alexander, B., Ault, A. P., Barth, M. C., Clegg, S. L., Collett Jr., J. L., Fahey, K. M., Hennigan, C. J., Herrmann, H., Kanakidou, M., Kelly, J. T., Ku, I., McNeill, V. F., Riemer, N., Schaefer, T., Shi, G., Tilgner, A., Walker, J. T., Wang, T., Weber, R., Xing, J., Zaveri, R. A., and Zuend, A.: The acidity of atmospheric particles and clouds, *Atmos. Chem. Phys.*, 20, 4809-4888, <http://doi.org/10.5194/acp-20-4809-2020>, 2020.

Ravishankara, A. R.: Heterogeneous and Multiphase Chemistry in the Troposphere, *Science*, 276, 1058-1064, <http://doi.org/10.1126/science.276.5315.1058>, 1997.

895 Ren, Y., Wei, J., Wu, Z., Ji, Y., Bi, F., Gao, R., Wang, X., Wang, G., and Li, H.: Chemical components and source identification of PM_{2.5} in non-heating season in Beijing: The influences of biomass burning and dust, *Atmos. Res.*, 251, 105412, <http://doi.org/10.1016/j.atmosres.2020.105412>, 2021.

Rindelaub, J. D., Craig, R. L., Nandy, L., Bondy, A. L., Dutcher, C. S., Shepson, P. B., and Ault, A. P.: Direct Measurement of pH in Individual Particles via Raman Microspectroscopy and Variation in Acidity with Relative Humidity, *J. Phys. Chem. A*, 120, 911-917, <http://doi.org/10.1021/acs.jpca.5b12699>, 2016.

Rossi, M. J.: Heterogeneous Reactions on Salts, *Chem. Rev.*, 103, 4823-4882, <http://doi.org/10.1021/cr020507n>, 2003.

Rubasinghege, G., and Grassian, V. H.: Role(s) of adsorbed water in the surface chemistry of environmental interfaces, *Chem. Commun.*, 49, 3071-3094, <http://doi.org/10.1039/C3CC38872G>, 2013.

900 Sakata, K., Takahashi, Y., Takano, S., Matsuki, A., Sakaguchi, A., and Tanimoto, H.: First X-ray Spectroscopic Observations of Atmospheric Titanium Species: Size Dependence and the Emission Source, *Environ. Sci. Technol.*, 55, 10975-10986, <http://doi.org/10.1021/acs.est.1c02000>, 2021.

Sarwar, G., Fahey, K., Kwok, R., Gilliam, R. C., Roselle, S. J., Mathur, R., Xue, J., Yu, J., and Carter, W. P. L.: Potential impacts of two SO₂ oxidation pathways on regional sulfate concentrations: Aqueous-phase oxidation by NO₂ and gas-phase oxidation by Stabilized Criegee Intermediates, *Atmos. Environ.*, 68, 186-197, <http://doi.org/10.1016/j.atmosenv.2012.11.036>, 2013.

910 Scheinhardt, S., Müller, K., Spindler, G., and Herrmann, H.: Complexation of trace metals in size-segregated aerosol particles at nine sites in Germany, *Atmos. Environ.*, 74, 102-109, <http://doi.org/10.1016/j.atmosenv.2013.03.023>, 2013.

Seinfeld, J. H., and Pandis, S. N.: *Atmospheric Chemistry and Physics, From Air Pollution to Climate Change*, 3rd Edition, Wiley, New Jersey, USA, 2016.

915 Shang, J., Li, J., and Zhu, T.: Heterogeneous reaction of SO₂ on TiO₂ particles, *Science China Chemistry*, 53, 2637-2643, <http://doi.org/10.1007/s11426-010-4160-3>, 2010.

Shao, J., Chen, Q., Wang, Y., Lu, X., He, P., Sun, Y., Shah, V., Martin, R. V., Philip, S., Song, S., Zhao, Y., Xie, Z., Zhang, L., and Alexander, B.: Heterogeneous sulfate aerosol formation mechanisms during wintertime Chinese haze events: air quality model assessment using observations of sulfate oxygen isotopes in Beijing, *Atmos. Chem. Phys.*, 19, 6107-6123, <http://doi.org/10.5194/acp-19-6107-2019>, 2019.

920 Shi, Z., Krom, M. D., Jickells, T. D., Bonneville, S., Carslaw, K. S., Mihalopoulos, N., Baker, A. R., and Benning, L. G.: Impacts on iron solubility in the mineral dust by processes in the source region and the atmosphere: A review, *Aeolian Res.*, 5, 21-42, <http://doi.org/10.1016/j.aeolia.2012.03.001>, 2012.

Song, H., Lu, K., Ye, C., Dong, H., Li, S., Chen, S., Wu, Z., Zheng, M., Zeng, L., Hu, M., and Zhang, Y.: A comprehensive observation-based multiphase chemical model analysis of sulfur dioxide oxidations in both summer and winter, *Atmos. Chem. Phys.*, 21, 13713-13727, <http://doi.org/10.5194/acp-21-13713-2021>, 2021.

925 Song, S., Nenes, A., Gao, M., Zhang, Y., Liu, P., Shao, J., Ye, D., Xu, W., Lei, L., Sun, Y., Liu, B., Wang, S., and McElroy,

930 M. B.: Thermodynamic Modeling Suggests Declines in Water Uptake and Acidity of Inorganic Aerosols in Beijing Winter Haze Events during 2014/2015–2018/2019, *Environ. Sci. Technol. Lett.*, 6, 752-760, <http://doi.org/10.1021/acs.estlett.9b00621>, 2019.

935 Stelson, A. W., and Seinfeld, J. H.: Chemical Mass Accounting of Urban Aerosol, *Environ. Sci. Technol.*, 15, 671-679, <http://doi.org/10.1021/es00088a005>, 1981.

940 Su, H., Cheng, Y., and Pöschl, U.: New Multiphase Chemical Processes Influencing Atmospheric Aerosols, Air Quality, and Climate in the Anthropocene, *Accounts Chem. Res.*, 53, 2034-2043, <http://doi.org/10.1021/acs.accounts.0c00246>, 2020.

945 Sullivan, R. C., Guazzotti, S. A., Sodeman, D. A., and Prather, K. A.: Direct observations of the atmospheric processing of Asian mineral dust, *Atmos. Chem. Phys.*, 7, 1213-1236, <http://doi.org/10.5194/acp-7-1213-2007>, 2007.

950 Tang, M., Cziezo, D. J., and Grassian, V. H.: Interactions of water with mineral dust aerosol: water adsorption, hygroscopicity, cloud condensation, and ice nucleation, *Chem. Rev.*, 116, 4205-4259, <http://doi.org/10.1021/acs.chemrev.5b00529>, 2016.

955 Tang, M., Huang, X., Lu, K., Ge, M., Li, Y., Cheng, P., Zhu, T., Ding, A., Zhang, Y., Gligorovski, S., Song, W., Ding, X., Bi, X., and Wang, X.: Heterogeneous reactions of mineral dust aerosol: implications for tropospheric oxidation capacity, *Atmos. Chem. Phys.*, 17, 11727-11777, <http://doi.org/10.5194/acp-17-11727-2017>, 2017.

960 Tang, M., Zhang, H., Gu, W., Gao, J., Jian, X., Shi, G., Zhu, B., Xie, L., Guo, L., Gao, X., Wang, Z., Zhang, G., and Wang, X.: Hygroscopic Properties of Saline Mineral Dust From Different Regions in China: Geographical Variations, Compositional Dependence, and Atmospheric Implications, *J. Geophys. Res.: Atmos.*, 124, 10844-10857, <http://doi.org/10.1029/2019JD031128>, 2019.

965 Tao, W., Su, H., Zheng, G., Wang, J., Wei, C., Liu, L., Ma, N., Li, M., Zhang, Q., Pöschl, U., and Cheng, Y.: Aerosol pH and chemical regimes of sulfate formation in aerosol water during winter haze in the North China Plain, *Atmos. Chem. Phys.*, 20, 11729-11746, <http://doi.org/10.5194/acp-20-11729-2020>, 2020.

970 Textor, C., Schulz, M., Guibert, S., Kinne, S., Balkanski, Y., Bauer, S., Berntsen, T., Berglen, T., Boucher, O., Chin, M., Dentener, F., Diehl, T., Easter, R., Feichter, H., Fillmore, D., Ghan, S., Ginoux, P., Gong, S., Grini, A., Hendricks, J., Horowitz, L., Huang, P., Isaksen, I., Iversen, T., Kloster, S., Koch, D., A. Kirkevag, Kristjansson, J. E., Krol, M., Lauer, A., Lamarque, J. F., Liu, X., Montanaro, V., Myhre, G., Penner, J., Pitari, G., Reddy, S., Seland, Ø., Stier, P., Takemura, T., and Tie, X.: Analysis and quantification of the diversities of aerosol life cycles within AeroCom, *Atmos. Chem. Phys.*, 6, 1777-1813, <http://doi.org/10.5194/acp-6-1777-2006>, 2006.

975 Tian, R., Ma, X., Sha, T., Pan, X., and Wang, Z.: Exploring dust heterogeneous chemistry over China: Insights from field observation and GEOS-Chem simulation, *Sci. Total Environ.*, 798, 149307, <http://doi.org/10.1016/j.scitotenv.2021.149307>, 2021.

Tilgner, A., Schaefer, T., Alexander, B., Barth, M., Collett Jr., J. L., Fahey, K. M., Nenes, A., Pye, H. O. T., Herrmann, H., and McNeill, V. F.: Acidity and the multiphase chemistry of atmospheric aqueous particles and clouds, *Atmos. Chem. Phys.*, 21, 13483-13536, <http://doi.org/10.5194/acp-21-13483-2021>, 2021.

Tutsak, E., and Koçak, M.: High time-resolved measurements of water-soluble sulfate, nitrate and ammonium in PM_{2.5} and their precursor gases over the Eastern Mediterranean, *Sci. Total Environ.*, 672, 212-226, <http://doi.org/10.1016/j.scitotenv.2019.03.451>, 2019.

Ullerstam, M., Johnson, M. S., Vogt, R., and Ljungstrom, E.: DRIFTS and Knudsen cell study of the heterogeneous reactivity of SO₂ and NO₂ on mineral dust, *Atmos. Chem. Phys.*, 3, 2043-2051, <http://doi.org/10.5194/acp-3-2043-2003>, 2003.

Ullerstam, M., Vogt, R., Langer, S., and Ljungström, E.: The kinetics and mechanism of SO₂ oxidation by O₃ on mineral dust, *Phys. Chem. Chem. Phys.*, 4, 4694-4699, <http://doi.org/10.1039/B203529B>, 2002.

Uno, I., Eguchi, K., Yumimoto, K., Takemura, T., Shimizu, A., Uematsu, M., Liu, Z., Wang, Z., Hara, Y., and Sugimoto, N.: Asian dust transported one full circuit around the globe, *Nat. Geosci.*, 2, 557-560, <http://doi.org/10.1038/ngeo583>, 2009.

Urupina, D., Gaudion, V., Romanias, M. N., Verrielle, M., and Thevenet, F.: Method development and validation for the determination of sulfites and sulfates on the surface of mineral atmospheric samples using reverse-phase liquid chromatography, *Talanta*, 219, 121318, <http://doi.org/10.1016/j.talanta.2020.121318>, 2020.

975 Urupina, D., Gaudion, V., Romanias, M. N., and Thevenet, F.: Surface Distribution of Sulfites and Sulfates on Natural Volcanic and Desert Dusts: Impact of Humidity and Chemical Composition, *ACS Earth Space Chem.*, 6, 642-655, <http://doi.org/10.1021/acsearthspacechem.1c00321>, 2022.

Urupina, D., Lasne, J., Romanias, M. N., Thiery, V., Dagsson-Waldhauserova, P., and Thevenet, F.: Uptake and surface chemistry of SO₂ on natural volcanic dusts, *Atmos. Environ.*, 217, 116942, <http://doi.org/10.1016/j.atmosenv.2019.116942>,

2019.

980 Urupina, D., Romanias, M. N., and Thevenet, F.: How Relevant Is It to Use Mineral Proxies to Mimic the Atmospheric Reactivity of Natural Dust Samples? A Reactivity Study Using SO₂ as Probe Molecule, *Minerals*, 11, 282, <http://doi.org/10.3390/min11030282>, 2021.

985 Usher, C. R., Al-Hosney, H., Carlos-Cuellar, S., and Grassian, V. H.: A laboratory study of the heterogeneous uptake and oxidation of sulfur dioxide on mineral dust particles, *J. Geophys. Res.: Atmos.*, 107, 4713, <http://doi.org/10.1029/2002JD002051>, 2002.

990 Usher, C. R., Michel, A. E., and Grassian, V. H.: Reactions on mineral dust, *Chem. Rev.*, 103, 4883-4940, <http://doi.org/10.1021/cr020657y>, 2003.

995 Volkamer, R., San Martini, F., Molina, L. T., Salcedo, D., Jimenez, J. L., and Molina, M. J.: A missing sink for gas-phase glyoxal in Mexico City: Formation of secondary organic aerosol, *Geophys. Res. Lett.*, 34, <http://doi.org/10.1029/2007GL030752>, 2007.

Wang, G., Zhang, R., Gomez, M. E., Yang, L., Levy Zamora, M., Hu, M., Lin, Y., Peng, J., Guo, S., Meng, J., Li, J., Cheng, C., Hu, T., Ren, Y., Wang, Y., Gao, J., Cao, J., An, Z., Zhou, W., Li, G., Wang, J., Tian, P., Marrero-Ortiz, W., Secretst, J., Du, Z., Zheng, J., Shang, D., Zeng, L., Shao, M., Wang, W., Huang, Y., Wang, Y., Zhu, Y., Li, Y., Hu, J., Pan, B., Cai, L., Cheng, Y., Ji, Y., Zhang, F., Rosenfeld, D., Liss, P. S., Duce, R. A., Kolb, C. E., and Molina, M. J.: Persistent sulfate formation from London Fog to Chinese haze, *Proc. Natl. Acad. Sci. U. S. A.*, 113, 13630-13635, <http://doi.org/10.1073/pnas.1616540113>, 2016.

1000 Wang, H., Zhong, C., Ma, Q., Ma, J., and He, H.: The adsorption and oxidation of SO₂ on MgO surface: experimental and DFT calculation studies, *Environ. Sci.: Nano*, 7, 1092-1101, <http://doi.org/10.1039/C9EN01474H>, 2020b.

1005 Wang, K., Hattori, S., Lin, M., Ishino, S., Alexander, B., Kamezaki, K., Yoshida, N., and Kang, S.: Isotopic constraints on atmospheric sulfate formation pathways in the Mt. Everest region, southern Tibetan Plateau, *Atmos. Chem. Phys.*, 21, 8357-8376, <http://doi.org/10.5194/acp-21-8357-2021>, 2021b.

1010 Wang, K., Zhang, Y., Nenes, A., and Fountoukis, C.: Implementation of dust emission and chemistry into the Community Multiscale Air Quality modeling system and initial application to an Asian dust storm episode, *Atmos. Chem. Phys.*, 12, 10209-10237, <http://doi.org/10.5194/acp-12-10209-2012>, 2012.

1015 Wang, R., Yang, N., Li, J., Xu, L., Tsona, N. T., Du, L., and Wang, W.: Heterogeneous reaction of SO₂ on CaCO₃ particles: Different impacts of NO₂ and acetic acid on the sulfite and sulfate formation, *J. Environ. Sci.*, <http://doi.org/10.1016/j.jes.2021.08.017>, 2022b.

1020 Wang, S., Wang, L., Fan, X., Wang, N., Ma, S., and Zhang, R.: Formation pathway of secondary inorganic aerosol and its influencing factors in Northern China: Comparison between urban and rural sites, *Sci. Total Environ.*, 840, 156404, <http://doi.org/10.1016/j.scitotenv.2022.156404>, 2022a.

1025 Wang, T., Liu, Y., Deng, Y., Cheng, H., Fang, X., and Zhang, L.: Heterogeneous Formation of Sulfur Species on Manganese Oxides: Effects of Particle Type and Moisture Condition, *J. Phys. Chem. A*, 124, 7300-7312, <http://doi.org/10.1021/acs.jpca.0c04483>, 2020d.

1030 Wang, T., Liu, Y., Deng, Y., Cheng, H., Yang, Y., Feng, Y., Zhang, L., Fu, H., and Chen, J.: Photochemical Oxidation of Water-Soluble Organic Carbon (WSOC) on Mineral Dust and Enhanced Organic Ammonium Formation, *Environ. Sci. Technol.*, 54, 15631-15642, <http://doi.org/10.1021/acs.est.0c04616>, 2020c.

1035 Wang, T., Liu, Y., Deng, Y., Fu, H., Zhang, L., and Chen, J.: The influence of temperature on the heterogeneous uptake of SO₂ on hematite particles, *Sci. Total Environ.*, 644, 1493-1502, <http://doi.org/10.1016/j.scitotenv.2018.07.046>, 2018a.

1040 Wang, T., Liu, Y., Deng, Y., Fu, H., Zhang, L., and Chen, J.: Emerging investigator series: heterogeneous reactions of sulfur dioxide on mineral dust nanoparticles: from single component to mixed components, *Environ. Sci.: Nano*, 5, 1821-1833, <http://doi.org/10.1039/C8EN00376A>, 2018b.

1045 Wang, T., Liu, Y., Deng, Y., Fu, H., Zhang, L., and Chen, J.: Adsorption of SO₂ on mineral dust particles influenced by atmospheric moisture, *Atmos. Environ.*, 191, 153-161, <http://doi.org/10.1016/j.atmosenv.2018.08.008>, 2018c.

1050 Wang, T., Liu, M., Liu, M., Song, Y., Xu, Z., Shang, F., Huang, X., Liao, W., Wang, W., Ge, M., Cao, J., Hu, J., Tang, G., Pan, Y., Hu, M., and Zhu, T.: Sulfate Formation Apportionment during Winter Haze Events in North China, *Environ. Sci. Technol.*, 56, 7771-7778, <http://doi.org/10.1021/acs.est.2c02533>, 2022c.

1055 Wang, W., Liu, M., Wang, T., Song, Y., Zhou, L., Cao, J., Hu, J., Tang, G., Chen, Z., Li, Z., Xu, Z., Peng, C., Lian, C., Chen, Y., Pan, Y., Zhang, Y., Sun, Y., Li, W., Zhu, T., Tian, H., and Ge, M.: Sulfate formation is dominated by manganese-

catalyzed oxidation of SO_2 on aerosol surfaces during haze events, *Nat. Commun.*, 12, 1993, <http://doi.org/10.1038/s41467-021-22091-6>, 2021a.

1030 1035 1040 1045 1050 1055 1060 1065 1070 1075

Wang, X., Gemayel, R., Hayeck, N., Perrier, S., Charbonnel, N., Xu, C., Chen, H., Zhu, C., Zhang, L., Wang, L., Nizkorodov, S. A., Wang, X., Wang, Z., Wang, T., Mellouki, A., Riva, M., Chen, J., and George, C.: Atmospheric Photosensitization: A New Pathway for Sulfate Formation, *Environ. Sci. Technol.*, 54, 3114-3120, <http://doi.org/10.1021/acs.est.9b06347>, 2020a.

Wang, Y., Zhang, Q., Jiang, J., Zhou, W., Wang, B., He, K., Duan, F., Zhang, Q., Philip, S., and Xie, Y.: Enhanced sulfate formation during China's severe winter haze episode in January 2013 missing from current models, *J. Geophys. Res.*, 119, 10425-10440, <http://doi.org/10.1002/2013jd021426>, 2014.

Wang, Z., Wang, T., Fu, H., Zhang, L., Tang, M., George, C., Grassian, V. H., and Chen, J.: Enhanced heterogeneous uptake of sulfur dioxide on mineral particles through modification of iron speciation during simulated cloud processing, *Atmos. Chem. Phys.*, 19, 12569-12585, <http://doi.org/10.5194/acp-19-12569-2019>, 2019.

Wu, C., Zhang, S., Wang, G., Lv, S., Li, D., Liu, L., Li, J., Liu, S., Du, W., Meng, J., Qiao, L., Zhou, M., Huang, C., and Wang, H.: Efficient Heterogeneous Formation of Ammonium Nitrate on the Saline Mineral Particle Surface in the Atmosphere of East Asia during Dust Storm Periods, *Environ. Sci. Technol.*, 54, 15622-15630, <http://doi.org/10.1021/acs.est.0c04544>, 2020.

Wu, L. Y., Tong, S. R., Wang, W. G., and Ge, M. F.: Effects of temperature on the heterogeneous oxidation of sulfur dioxide by ozone on calcium carbonate, *Atmos. Chem. Phys.*, 11, 6593-6605, <http://doi.org/10.5194/acp-11-6593-2011>, 2011.

Wu, L., Tong, S., Zhou, L., Wang, W., and Ge, M.: Synergistic effects between SO_2 and HCOOH on $\alpha\text{-Fe}_2\text{O}_3$, *J. Phys. Chem. A*, 117, 3972-3979, <http://doi.org/10.1021/jp400195f>, 2013.

Xu, M., Qiu, P., He, Y., Guo, S., Bai, Y., Zhang, H., Zhao, S., Shen, X., Zhu, B., Guo, Q., and Guo, Z.: Sulfur isotope composition during heterogeneous oxidation of SO_2 on mineral dust: The effect of temperature, relative humidity, and light intensity, *Atmos. Res.*, 254, 105513, <http://doi.org/10.1016/j.atmosres.2021.105513>, 2021.

Xu, W., Kuang, Y., Liang, L., He, Y., Cheng, H., Bian, Y., Tao, J., Zhang, G., Zhao, P., Ma, N., Zhao, H., Zhou, G., Su, H., Cheng, Y., Xu, X., Shao, M., and Sun, Y.: Dust-Dominated Coarse Particles as a Medium for Rapid Secondary Organic and Inorganic Aerosol Formation in Highly Polluted Air, *Environ. Sci. Technol.*, 54, 15710-15721, <http://doi.org/10.1021/acs.est.0c07243>, 2020.

Xue, J., Yuan, Z., Griffith, S. M., Yu, X., Lau, A. K. H., and Yu, J. Z.: Sulfate formation enhanced by a cocktail of high NO_x , SO_2 , particulate matter, and droplet pH during haze-fog events in megacities in China: an observation-based modeling investigation, *Environ. Sci. Technol.*, 50, 7325-7334, <http://doi.org/10.1021/acs.est.6b00768>, 2016.

Yang, L., Yu, L. E., and Ray, M. B.: Degradation of paracetamol in aqueous solutions by TiO_2 photocatalysis, *Water Res.*, 42, 3480-3488, <http://doi.org/10.1016/j.watres.2008.04.023>, 2008.

Yang, N., Tsона, N. T., Cheng, S., Li, S., Xu, L., Wang, Y., Wu, L., and Du, L.: Competitive reactions of SO_2 and acetic acid on $\alpha\text{-Al}_2\text{O}_3$ and CaCO_3 particles, *Sci. Total Environ.*, 699, 134362, <http://doi.org/10.1016/j.scitotenv.2019.134362>, 2020.

Yang, W., Chen, M., Xiao, W., Guo, Y., Ding, J., Zhang, L., and He, H.: Molecular Insights into NO-Promoted Sulfate Formation on Model TiO_2 Nanoparticles with Different Exposed Facets, *Environ. Sci. Technol.*, 52, 14110-14118, <http://doi.org/10.1021/acs.est.8b02688>, 2018a.

Yang, W., He, H., Ma, Q., Ma, J., Liu, Y., Liu, P., and Mu, Y.: Synergistic formation of sulfate and ammonium resulting from reaction between SO_2 and NH_3 on typical mineral dust, *Phys. Chem. Chem. Phys.*, 18, 956-964, <http://doi.org/10.1039/C5CP06144J>, 2016.

Yang, W., Ma, Q., Liu, Y., Ma, J., Chu, B., Wang, L., and He, H.: Role of NH_3 in the Heterogeneous Formation of Secondary Inorganic Aerosols on Mineral Oxides, *J. Phys. Chem. A*, 122, 6311-6320, <http://doi.org/10.1021/acs.jpca.8b05130>, 2018b.

Yang, W., Ma, Q., Liu, Y., Ma, J., Chu, B., and He, H.: The effect of water on the heterogeneous reactions of SO_2 and NH_3 on the surfaces of $\alpha\text{-Fe}_2\text{O}_3$ and $\gamma\text{-Al}_2\text{O}_3$, *Environ. Sci.: Nano*, 6, 2749-2758, <http://doi.org/10.1039/C9EN00574A>, 2019.

Yang, W., Zhang, J., Ma, Q., Zhao, Y., Liu, Y., and He, H.: Heterogeneous reaction of SO_2 on manganese oxides: the effect of crystal structure and relative humidity, *Sci. Rep.-UK*, 7, 4550, <http://doi.org/10.1038/s41598-017-04551-6>, 2017.

Ye, C., Liu, P., Ma, Z., Xue, C., Zhang, C., Zhang, Y., Liu, J., Liu, C., Sun, X., and Mu, Y.: High H_2O_2 Concentrations Observed during Haze Periods during the Winter in Beijing: Importance of H_2O_2 Oxidation in Sulfate Formation, *Environ. Sci. Technol. Lett.*, 5, 757-763, <http://doi.org/10.1021/acs.estlett.8b00579>, 2018.

Yin, Z., Wan, Y., Zhang, Y., and Wang, H.: Why super sandstorm 2021 in North China, *Natl. Sci. Rev.*,

http://doi.org/10.1093/nsr/nwab165, 2021.

1080 Yu, J.: An interfacial role for NO_2 , *Nat. Chem.*, 13, 1158-1160, http://doi.org/10.1038/s41557-021-00845-5, 2021.

Yu, T., Zhao, D., Song, X., and Zhu, T.: NO_2 -initiated multiphase oxidation of SO_2 by O_2 on CaCO_3 particles, *Atmos. Chem. Phys.*, 18, 6679-6689, http://doi.org/10.5194/acp-18-6679-2018, 2018.

1085 Yu, Z., Jang, M., and Park, J.: Modeling atmospheric mineral aerosol chemistry to predict heterogeneous photooxidation of SO_2 , *Atmos. Chem. Phys.*, 17, 10001-10017, http://doi.org/10.5194/acp-17-10001-2017, 2017.

Zhang, F., Wang, Y., Peng, J., Chen, L., Sun, Y., Duan, L., Ge, X., Li, Y., Zhao, J., Liu, C., Zhang, X., Zhang, G., Pan, Y., Wang, Y., Zhang, A. L., Ji, Y., Wang, G., Hu, M., Molina, M. J., and Zhang, R.: An unexpected catalyst dominates formation and radiative forcing of regional haze, *Proc. Natl. Acad. Sci. U. S. A.*, 117, 3960-3966, http://doi.org/10.1073/pnas.1919343117, 2020.

1090 Zhang, H., Xu, Y., and Jia, L.: A chamber study of catalytic oxidation of SO_2 by $\text{Mn}^{2+}/\text{Fe}^{3+}$ in aerosol water, *Atmos. Environ.*, 245, 118019, http://doi.org/10.1016/j.atmosenv.2020.118019, 2021.

Zhang, R., Wang, G., Guo, S., Zamora, M. L., Ying, Q., Lin, Y., Wang, W., Hu, M., and Wang, Y.: Formation of urban fine particulate matter, *Chem. Rev.*, 115, 3803-3855, http://doi.org/10.1021/acs.chemrev.5b00067, 2015.

1095 Zhang, S., Xing, J., Sarwar, G., Ge, Y., He, H., Duan, F., Zhao, Y., He, K., Zhu, L., and Chu, B.: Parameterization of heterogeneous reaction of SO_2 to sulfate on dust with coexistence of NH_3 and NO_2 under different humidity conditions, *Atmos. Environ.*, 208, 133-140, http://doi.org/10.1016/j.atmosenv.2019.04.004, 2019a.

Zhang, X. Y., Wang, Y. Q., Niu, T., Zhang, X. C., Gong, S. L., Zhang, Y. M., and Sun, J. Y.: Atmospheric aerosol compositions in China: spatial/temporal variability, chemical signature, regional haze distribution and comparisons with global aerosols, *Atmos. Chem. Phys.*, 12, 779-799, http://doi.org/10.5194/acp-12-779-2012, 2012.

1100 Zhang, X., Zhuang, G., Chen, J., Wang, Y., Wang, X., An, Z., and Zhang, P.: Heterogeneous reaction of sulfur dioxide on typical mineral particles, *J. Phys. Chem. B*, 110, 12588-12596, http://doi.org/10.1021/jp0617773, 2006.

Zhang, Y., Bao, F., Li, M., Chen, C., and Zhao, J.: Nitrate-Enhanced Oxidation of SO_2 on Mineral Dust: A Vital Role of a Proton, *Environ. Sci. Technol.*, 53, 10139-10145, http://doi.org/10.1021/acs.est.9b01921, 2019b.

1105 Zhang, Y., Tong, S. R., and Ge, M. F.: A study about the influence of the size of CaCO_3 on the heterogeneous oxidation of sulfur dioxide by ozone, *Spectrosc. Spect. Anal.*, 36, 126-127, 2016.

Zhang, Y., Tong, S., Ge, M., Jing, B., Hou, S., Tan, F., Chen, Y., Guo, Y., and Wu, L.: The influence of relative humidity on the heterogeneous oxidation of sulfur dioxide by ozone on calcium carbonate particles, *Sci. Total Environ.*, 633, 1253-1262, http://doi.org/10.1016/j.scitotenv.2018.03.288, 2018.

1110 Zhanzakova, A., Tong, S., Yang, K., Chen, L., Li, K., Fu, H., Wang, L., and Kong, L.: The effects of surfactants on the heterogeneous uptake of sulfur dioxide on hematite, *Atmos. Environ.*, 213, 548-557, http://doi.org/10.1016/j.atmosenv.2019.06.050, 2019.

Zhao, D., Song, X., Zhu, T., Zhang, Z., and Liu, Y.: Multiphase oxidation of SO_2 by NO_2 on CaCO_3 particles, *Atmos. Chem. Phys.*, 18, 2481-2493, http://doi.org/10.5194/acp-2017-610, 2018.

1115 Zhao, X., Kong, L., Sun, Z., Ding, X., Cheng, T., Yang, X., and Chen, J.: Interactions between heterogeneous uptake and adsorption of sulfur dioxide and acetaldehyde on hematite, *J. Phys. Chem. A*, 119, 4001-4008, http://doi.org/10.1021/acs.jpca.5b01359, 2015.

Zheng, B., Zhang, Q., Zhang, Y., He, K. B., Wang, K., Zheng, G. J., Duan, F. K., Ma, Y. L., and Kimoto, T.: Heterogeneous chemistry: a mechanism missing in current models to explain secondary inorganic aerosol formation during the January 2013 haze episode in North China, *Atmos. Chem. Phys.*, 15, 2031-2049, http://doi.org/10.5194/acp-15-2031-2015, 2015.

1120 Zheng, H., Song, S., Sarwar, G., Gen, M., Wang, S., Ding, D., Chang, X., Zhang, S., Xing, J., Sun, Y., Ji, D., Chan, C. K., Gao, J., and McElroy, M. B.: Contribution of Particulate Nitrate Photolysis to Heterogeneous Sulfate Formation for Winter Haze in China, *Environ. Sci. Technol. Lett.*, http://doi.org/10.1021/acs.estlett.0c00368, 2020.

Zheng, S., Huang, Q., Zhou, J., and Wang, B.: A study on dye photoremoval in TiO_2 suspension solution, *Journal of photochemistry and photobiology. A, Chemistry.*, 108, 235-238, http://doi.org/10.1016/S1010-6030(97)00014-2, 1997.

Zhou, L., Wang, W., Gai, Y., and Ge, M.: Knudsen cell and smog chamber study of the heterogeneous uptake of sulfur dioxide on Chinese mineral dust, *J. Environ. Sci.*, 26, 2423-2433, http://doi.org/10.1016/j.jes.2014.04.005, 2014.

1125 Zhu, Y., Toon, O. B., Jensen, E. J., Bardeen, C. G., Mills, M. J., Tolbert, M. A., Yu, P., and Woods, S.: Persisting volcanic ash particles impact stratospheric SO_2 lifetime and aerosol optical properties, *Nat. Commun.*, 11, 4526, http://doi.org/10.1038/s41467-020-18352-5, 2020.